

The Promise of Regeneration: MSCs and Exosomes in Modern Medicine

Simplifying Progress

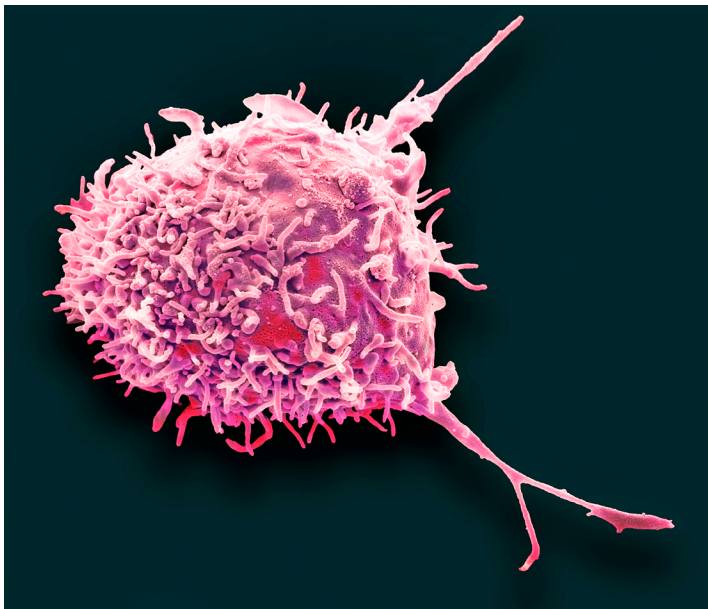


SARTORIUS

The Burden of Chronic Disease

A major challenge for modern medicine is the prevalence of chronic diseases in the population; conditions which for the most part cannot be cured but instead must be managed through medications and behavioural interventions. These diseases have a profound effect on patients' quality of life, especially those that are accompanied by progressive deterioration of tissue damage and organ function, such as autoimmune disorders, cardiovascular diseases, and musculoskeletal conditions including arthritis. These diseases not only cause physical pain and disability but also impose a heavy emotional and financial burden on patients, families, and healthcare systems.

Current treatment options for chronic diseases are often limited to symptom management using pain relievers, anti-inflammatory drugs, and immunosuppressants which can provide temporary relief but fail to address the underlying causes of inflammation, immunological dysfunction, and tissue damage. Given these limitations, there is a clear need for innovative therapies that can restore cells and tissues at the root of such conditions.



The Promise of Regenerative Medicine

The emergent field of regenerative medicine focuses on repair and replacement of damaged or diseased cells and tissues to reestablish normal functionality. It encompasses a range of strategies that aim to directly repair tissues, harness existing physiological systems to promote regeneration, or modulate immune responses.

Mesenchymal stem cells (MSCs) are adult stem cells that, having the capacity to differentiate into multiple cell types including bone, cartilage, muscle, and fat, have evident potential in treating a wide range of musculoskeletal disorders. They can be administered directly as stem cells into an area of interest, with the intention for them to spontaneously differentiate into the required cell types, or they can be directed in the lab to terminally differentiated cell types for introduction into the site of interest. Furthermore, their inherent immunomodulatory properties make them suitable candidates for the treatment of inflammatory and autoimmune diseases. MSCs as cell therapies have achieved regulatory approval, with many clinical trials currently in progress.¹

The mechanism for immunomodulation by MSCs is partly through cell-cell contact, but is partially mediated by extracellular vesicles (exosomes, or EVs). These cell-secreted particles play a crucial role in cell-to-cell communication and carry a cargo that can influence the behavior of recipient cells. Multiple studies have shown that application of EVs alone can replicate the cellular effects of MSCs, by virtue of their composition including effector proteins, genetic material, and cytokines. In some circumstances, using exosomes as therapeutics has advantages over cell products due to fewer logistical constraints, fewer off-target effects, and no requirement for host and donor matching.²

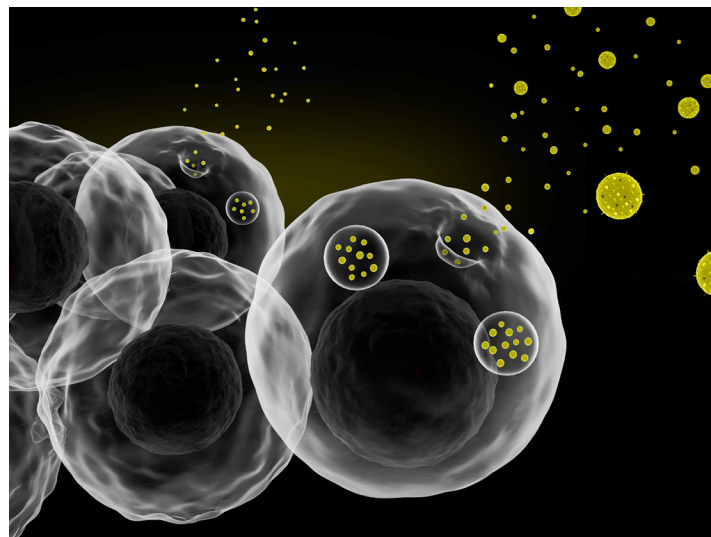
Advancing Regenerative Medicine

A major challenge in bringing these strategies to the clinic is the standardization of MSC and exosome production.³ Variability in cell sources, isolation methods, and culture conditions can affect the quality and effectiveness of these therapies. Establishing standardized protocols and rigorous quality control measures is essential to ensure consistent and reproducible results in clinical applications.

Similarly, ensuring that the potency and efficacy of MSCs and exosomes is of vital importance, including full characterization and understanding of mechanisms of action. Advanced analytical techniques are required to obtain a holistic picture of cell and exosome quality prior to patient administration.

Despite these challenges, the potential of MSCs and exosomes in regenerative medicine is immense. Advanced cell culture systems and biomanufacturing technologies are paving the way for large-scale production and clinical translation of these therapies. Sartorius is taking a leading role in addressing these challenges by offering analytical solutions that optimize R&D workflows and provide translational insights. By harnessing the regenerative and immunomodulatory properties of MSCs and the potent signaling capabilities of exosomes, researchers are able to develop innovative treatments that could transform the landscape of medicine.

This ebook brings together four application notes introducing Sartorius technologies that can bring value to regenerative medicine development workflows. Powerful analytics techniques can improve the quality of MSC populations for research and clinical applications, as well as confirming functionality. Exosome preparation can be enhanced by combining immuno-affinity chromatography with filtration, and live-cell analysis can be used to observe biological mechanisms of action.



References

1. D. Hoang, P. Pham, T. Bach, A. Ngo, Q. Nguyen, T. Phan, G. Nguyen, P. Le, V. Hoang, N. Forsyth, M. Heke and L. Nguyen, "Stem cell-based therapy for human diseases," *Sig Transduct Target Ther*, vol. 7, no. 272, 2022.
2. F. Tan, X. Li, Z. Wang, J. Li, K. Shahzad and J. Zheng, "Clinical applications of stem cell-derived exosomes," *Sig Transduct Target Ther*, vol. 9, no. 17, 2024.
3. A. Wilson, N. Brown, E. Rand and P. Genever, "Attitudes Towards Standardization of Mesenchymal Stromal Cells—A Qualitative Exploration of Expert Views," *Stem Cells Translational Medicine*, vol. 12, no. 11, p. 745–757, 2023.

Table of Contents

The Promise of Regeneration: MSCs and Exosomes in Modern Medicine

05

Elevate MSC Quality Standards With a Combined Live-Cell Analysis and HTS Cytometry Approach

13

Rapid Assessment of MSC Differentiation with Non-Invasive Monitoring and HTS Cytometry

24

Harnessing Exosomes for Biomedical Applications: Insights into Extracellular Vesicle Labeling and Cellular Uptake Using Live-Cell Analysis

32

Combining Immuno-Affinity Chromatography and Filtration to Improve Specificity and Size Distribution of Exosome-Containing EV Populations

Keywords or phrases:

Mesenchymal stem cells, Senescence, Regenerative Medicine, Tissue Engineering, Live-Cell Analysis, High Throughput Screening by Cytometry, Quality Control

Elevate MSC Quality Standards With a Combined Live-Cell Analysis and HTS Cytometry Approach


Authors: Natasha Lewis, Jasmine Trigg, Daryl Cole, Nicola Bevan
Sartorius UK Ltd, Royston, Hertfordshire, UK

Correspondence
Email: askascientist@sartorius.com

Abstract

Mesenchymal stem cells (MSCs) are pivotal in regenerative medicine and cell therapy due to their multipotent nature and immunomodulatory functions. Ensuring the quality of MSCs is crucial for their therapeutic efficacy, particularly in high-risk clinical applications. Challenges in evaluating MSC quality arise from donor variability, culture conditions, and passage numbers. Traditional endpoint assays fall short in providing dynamic insights, necessitating advanced technologies including live-cell analysis and high-throughput screening (HTS) cytometry, which offer real-time, high-throughput, and multiparametric analysis capabilities, addressing these challenges effectively.

Here, these techniques are used to demonstrate that MSC growth dynamics slow with age, with later passages showing reduced proliferation and increased senescence, as indicated by senescence-associated β -Galactosidase (SA- β -Gal) activity and morphological changes. Marker expression remains relatively stable, emphasizing the importance of utilizing multiparametric techniques for a holistic view of MSC quality.

 For further information, visit [sartorius.com](https://www.sartorius.com)

Introduction

Mesenchymal stem cells (MSCs) are multipotent cells that give rise to multiple tissue lineages including bone, cartilage, and fat. They are also a major component of the bone marrow hematopoietic stem cell niche and have both paracrine and immunomodulatory functions. As such, they are a key target cell type for cell therapies and tissue engineering research, including for mitigating adverse effects associated with cancer treatments,¹ in neuro-regeneration during treatment for ischemic stroke,² and as the source of MSC-derived exosomes in fracture healing.³

The therapeutic efficacy of MSCs is highly dependent on their quality. To this end, ensuring the quality of MSC cultures before administration as a cell therapy, either in stem cell or differentiated form, is of fundamental importance.

Accordingly, the minimum criteria as defined by the International Society for Cellular Therapy (ISCT)⁴ states that MSCs must be plastic-adherent when maintained in standard culture conditions, have a distinct marker expression profile (CD105, CD73 and CD90 positive, CD45 and CD34 negative), and have tri-lineage differentiation potential. Consistency within the population of interest, and retention of these properties along with self-renewal capacity all need to be confirmed before cells can be used for downstream applications.

During MSC culture, it is important to understand growth dynamics, multipotency, and level of senescence to ensure the highest quality MSCs are taken forward for subsequent

applications, especially in a high-risk clinical situation such as cell therapy. General consensus defines cell senescence as a permanent state of growth arrest without concurrent cell death. Biologically, it serves as a protective mechanism against the proliferation of damaged cells which could lead to tumorigenesis. However, in the context of cell therapy and quality control, senescent MSCs are undesirable due to their reduced efficacy, impaired differentiation potential, and altered secretory profile which could lead to unwanted pro-inflammatory or dysregulated microenvironments. Indicators of cellular senescence include increased doubling time, altered cell morphology, and senescence-associated β -Galactosidase (SA- β -Gal) activity.

Evaluating MSC quality presents several challenges. Firstly, MSCs can be derived from different donors and tissues, which leads to inherent variability of samples, influenced by donor age, health status, and genetic background. Additionally, variations in culture conditions, passage number, and the heterogeneity of MSC populations add further complications. Traditional methods for assessing MSC quality are often endpoint assays, providing limited information on dynamic processes. The use of advanced technologies such as the Incucyte® Live-Cell Analysis System and iQue® (HTS) cytometer platform can help overcome some of these challenges by providing real-time, rapid, and multiparametric analysis capabilities.

Materials and Methods

Media for Routine Cell Culture

Materials	Supplier	Cat. No.
MSC NutriStem® XF Medium	Sartorius	05-200-1A
MSC NutriStem® XF Supplement Mix	Sartorius	05-201-1U
NutriCoat™ Attachment Solution	Sartorius	05-760-1-15
Bone marrow Mesenchymal stem cells RoosterVial™-hBM	RoosterBio	MSC-003

Table 1. Cell Culture Media and Reagents Used for Culturing MSCs

Surface Marker Expression Panel Reagents

	Product Name	Supplier	Cat. No.	Final Concentration
Viability	Zombie Violet™ Fixable Viability Kit	BioLegend	423113	1:200
MSC marker panel	PE Dazzle™ 594 anti-human CD90 (Thy1) Antibody	BioLegend	328133	1:100
	PE Cyanine7 anti-human CD105 Antibody	BioLegend	323217	1:100
	APC anti-human CD73 (Ecto-5'-nucleotidase) Antibody	BioLegend	344005	1:100
	Brilliant Violet 570™ anti-human CD45 Antibody	BioLegend	304033	1:100
	FITC anti-human CD34 Antibody	Invitrogen	MA5-16925	1:100
Senescence	Senescence Assay Kit (Beta Galactosidase, Fluorescence)	Abcam	ab228562	1:333

Table 2. Reagents Used for Cell Analysis Using the iQue® HTS Cytometer

MSC Culture

Prior to seeding into culture vessels for routine culture and experiments, plates and flasks were pre-coated with NutriCoat™ Attachment Solution. The solution was diluted 1:500 in PBS according to the manufacturer's instructions. The diluted coating solution was added to the culture vessel and incubated for 1 hour in a humidified CO₂ incubator (37°C). Prior to cell seeding, the solution was aspirated, and cell culture media containing a cell suspension was quickly added to ensure that the coating did not dry out.

MSCs were obtained from RoosterBio and cultured in MSC Nutristem® XF basal medium. They were seeded at a density of 3K cells/cm² in tissue culture flasks and passaged at 80% confluency and analyzed using the Incucyte® System. Cell confluence was measured using integrated Incucyte® AI Confluence Analysis.

Surface Marker Expression

MSCs were harvested at passage and analyzed for expression of markers CD34, CD45, CD73, CD90, and CD105. Following harvest, cells were washed in PBS and stained for viability using Zombie Violet™ for 20 minutes in the dark at room temperature. The cells were seeded into a 96-well V-bottom plate at 20K/well and washed twice with PBS + 2% FBS before staining with the MSC marker antibody cocktail as described in Table 2 for 30 minutes at room temperature. The cells were washed twice by centrifugation (5 min at 1000 × g) using PBS + 2% FBS. Cells were then resuspended in 20 µL of PBS + 2% FBS and analyzed on the iQue® HTS Cytometer. Data was analyzed using integrated iQue Forecyt® Software.

MSC Senescence Analysis

MSCs were seeded into a 24-well plate at 10K/well and cultured until 80% confluent. The media was removed and replenished with media containing 1.5 µL Senescence Dye per 500 µL media. Following a 2 hour incubation at 37°C, the cells were scanned in the Incucyte to collect images for quantification, washed twice in Assay Buffer XXVII | Wash Buffer, then harvested by trypsinization, washed, and resuspended for analysis on the iQue® HTS Platform.

Unstained cells were used as a negative control. Label-free quantification of images was performed using the Incucyte® AI Cell Health Analysis Software Module, which enables AI-based segmentation of heterogeneous cell morphologies to give univariate morphology metrics (AI Cell Segmentation).

Results

Reduction in MSC Growth Rate is Linked to Cellular Age

One key measure of MSC functionality is their proliferative capacity. Monitoring percentage confluence over time provides valuable insights into the growth dynamics of MSCs across different passages and under various culture conditions.

Live-cell analysis can be utilized to compare the proliferation of MSCs during routine culture under different conditions and over multiple passages. Cells were initially thawed in commercially available medium, then cultured in parallel in the commercial medium and in MSC NutriStem® XF medium. In MSCs cultured in a commercially available MSC medium (Figure 1A), the time required to reach confluence increased noticeably with passage number. Specifically, cells at passages 1 and 2 (P1 and P2) achieved 80% confluence within 3 days.

In contrast, cells at passage 3 (P3) required over 6 days to reach the same confluence, and cells at passage 4 (P4) only reached 70% confluence after 12 days.

For comparison, MSCs cultured in MSC NutriStem® XF medium (Figure 1B) exhibited a similar trend of slowing growth rates as the cells aged. Cells at P2 and P3 maintained a high proliferative capacity, rapidly reaching confluence within 4 days. Mid-passage cells (P4–P6) showed a decline in growth rate, achieving 80% confluence within 6–7 days. Late passage cells (P7) demonstrated a significant reduction in proliferation, with confluence remaining below 50% even after 7 days of culture. This suggests that these cells may have entered a state of growth arrest or senescence.

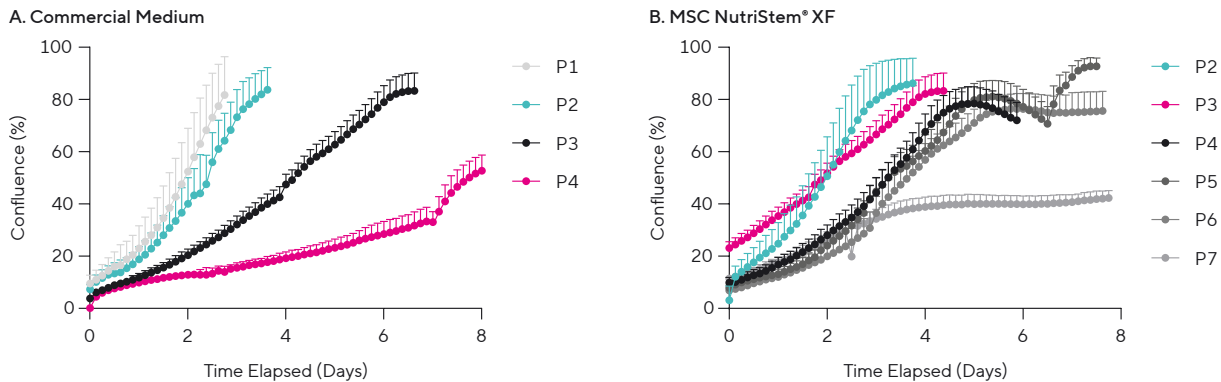


Figure 1. MSC Percentage Confluence Over Time During Routine Culture, Evaluated Using Live-Cell Analysis.
(A) MSCs cultured in a commercially available medium. (B) MSCs cultured in MSC NutriStem® XF medium.

Expression of MSC Identifying Markers Does Not Significantly Alter With Age

As mentioned previously, MSCs can be defined as having a distinct expression pattern for five markers, i.e., positive for CD73, CD90, and CD105, and negative for CD34 and CD45. Analysis of the percentage positive population for each of these markers for MSCs at passages 1–6 (Figure 2) show that the expected positive markers remain highly expressed even by older cells.

The levels of CD34 and CD45 positivity are slightly elevated in the later passages, suggesting some loss of multipotency. However, the minimal changes in marker expression suggest that this is insufficient alone to determine cell quality and should be evaluated in combination with other factors.

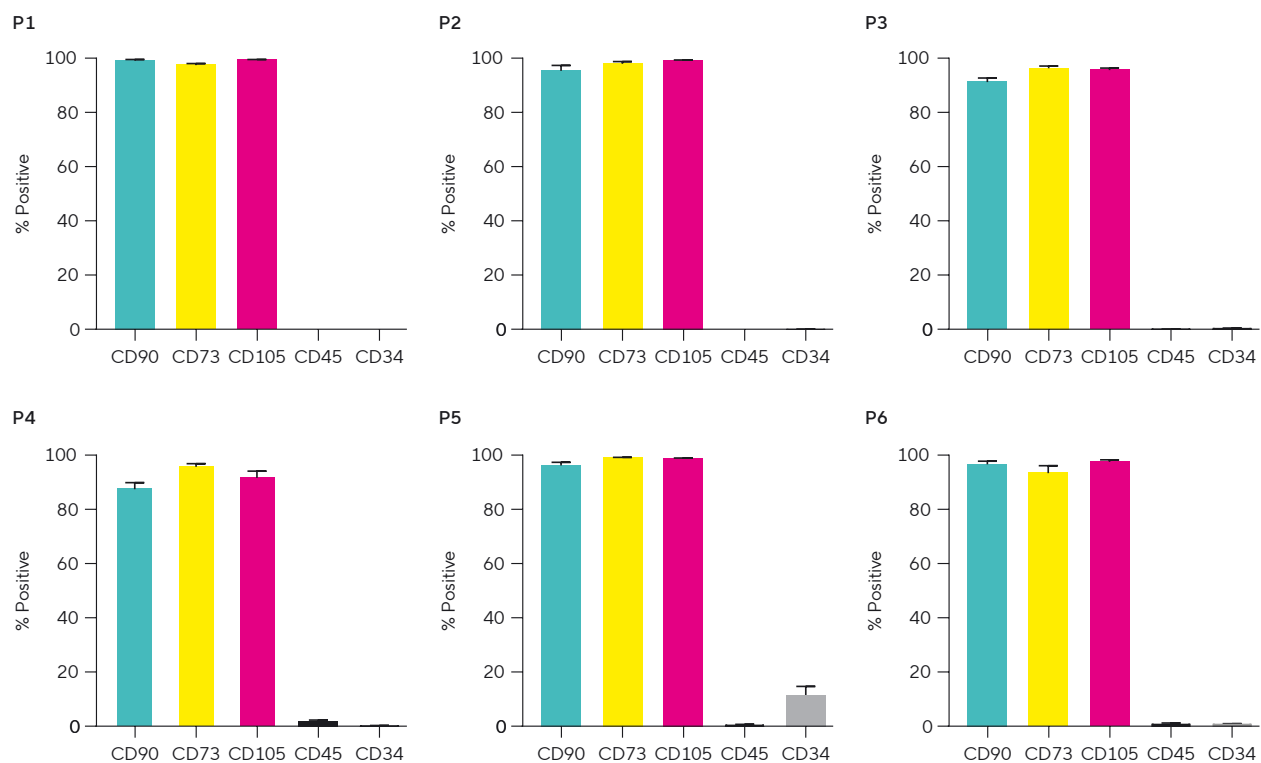


Figure 2. Expression of MSC Marker Panel Over Multiple Passages. Percentage positive populations are shown for each marker, as measured using HTS cytometry. Data shows percentage populations of an average of flasks at each passage, cultured in both Nutristem® and in commercial medium.

Multiparametric Evaluation Demonstrates That MSC Senescence Increases With Age

Evaluating MSC morphology can also provide valuable insights into cell status. MSCs tend to become larger and more irregular in shape as they age, indicated by a flattened, elongated shape with increased cytoplasmic area and granularity. In contrast, young MSCs are typically spindle-shaped and have a high nucleus-to-cytoplasm ratio.⁵

From the images, this difference is evident with cells in the earlier passages exhibiting smaller cell bodies which tend to increase gradually in size as the cells age through to P6 (Figure 3A). This morphology can also be indicative of a senescent state.

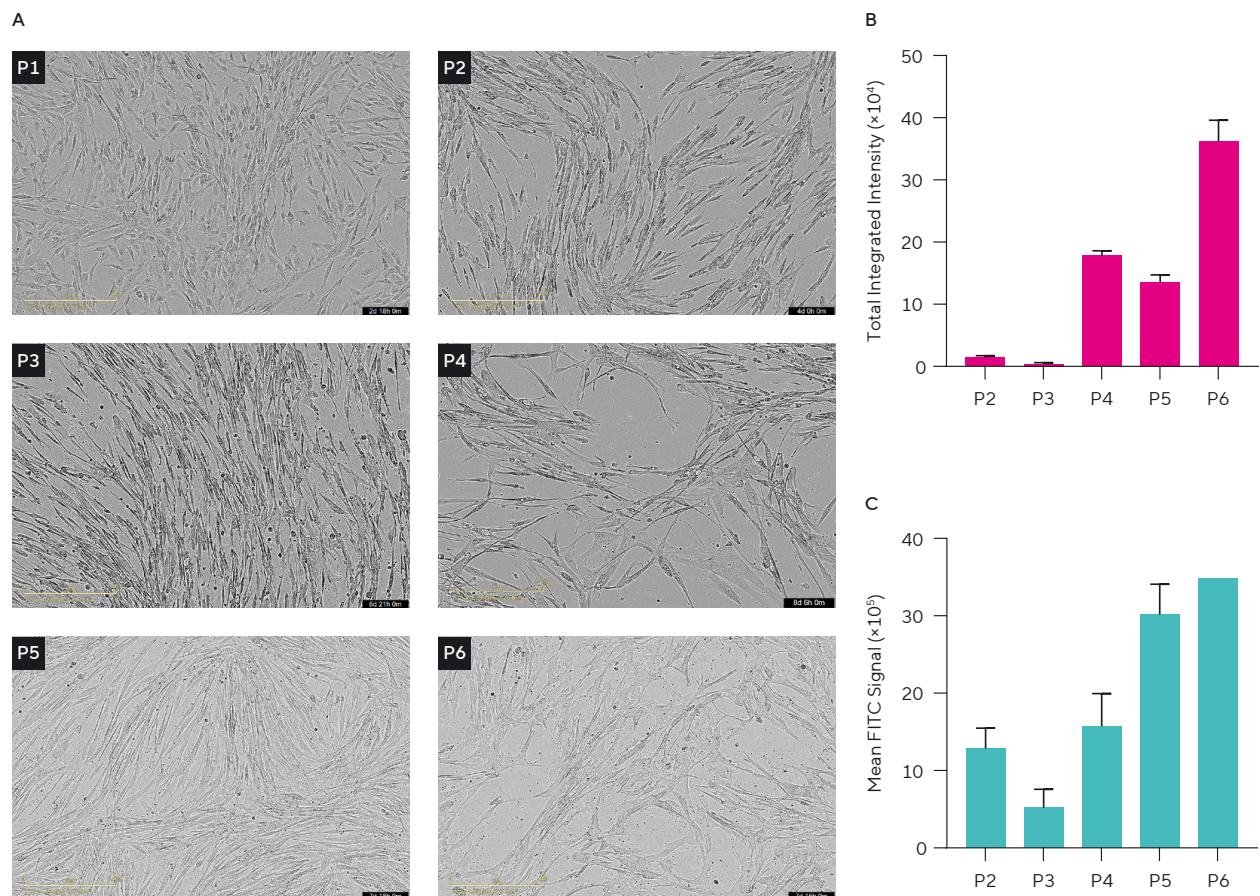


Figure 3. MSC Morphology and Quantification of Senescence Over Multiple Passages. (A) Images of MSCs at passages 1–6 at point of harvest. (B) Quantification of MSC senescence by analysis of fluorescent SA- β -Gal activity using live-cell analysis. (C) Quantification of MSC senescence by analysis of fluorescent SA- β -Gal activity of single cells using HTS cytometry.

Cellular senescence can be quantified through measuring SA- β -Gal activity at pH 6. In this study, fluorescent SA- β -Gal has been measured using both live-cell imaging (Figure 3B) and single cell fluorescence detection using HTS cytometry (Figure 3C). The data sets presented here were generated using the same samples. Although both analysis methods show similar trends, with fluorescent SA- β -Gal activity increasing with increased passage number as expected, the data obtained using live-cell analysis portray a clearer difference between the early and late passage cells. This could be linked to the different detection systems in each instrument; the optical path (including filters, lenses, and detectors), and the calibration or sensitivity level may affect the amount of fluorescence detected.

Label-free analysis can aid in the evaluation of MSC quality and hence senescence, by quantifying cell morphology through various metrics. Analysis of the images demonstrate both average cell area (Figure 4A) and eccentricity (Figure 4B) change as passage number and the age of the cells increase.

The data presented was taken from cells that were at the same percentage confluence (30%) to account for the changes in cell morphology and barriers to efficient cell segmentation as cells reach high confluence.

In accordance with expectations, these metrics indicate an increased cell size and increased irregularity in cell shape as the cells approach the Hayflick limit – the number of times a cell will divide before proliferation stops. The Hayflick limit is a particular consideration in the use of MSCs for therapeutic purposes, as it affects their proliferative capacity and longevity. These metrics provide researchers, looking to preserve valuable cellular material, with the potential to quantify the quality of MSCs label-free without having to employ labor-intensive and destructive protocols.

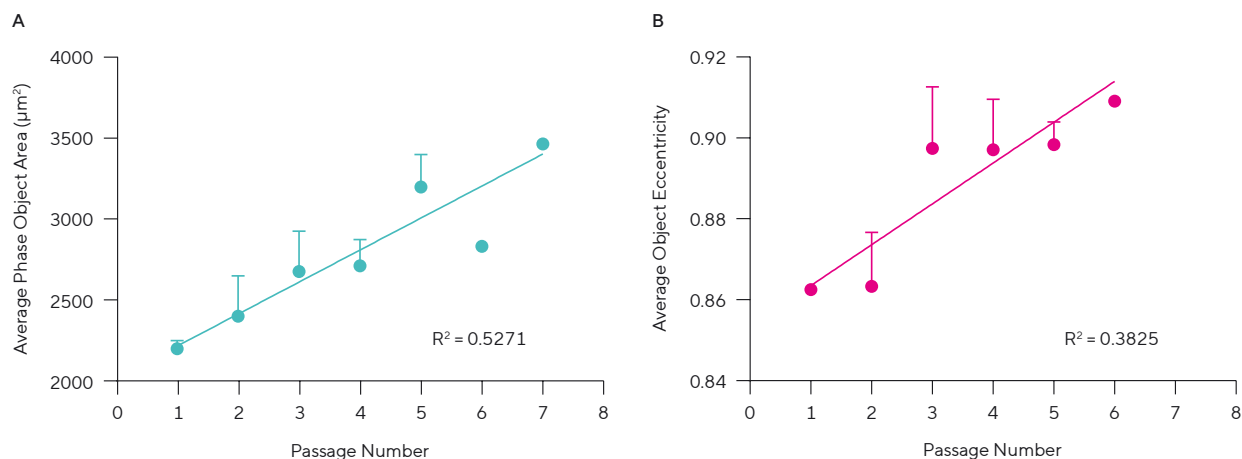


Figure 4. Quantification of MSC Morphological Characteristics Using Live-Cell Analysis. (A) Average cell area at 30% confluence. (B) Average cell eccentricity at 30% confluence.

Summary and Outlook

In conclusion, the combined use of live-cell analysis and HTS cytometry represents a powerful and effective strategy for the thorough evaluation of MSC quality and functionality. This integrated workflow not only improves the standardization and reproducibility of MSC assessments but also supports the advancement of MSC research and clinical applications.

By leveraging the strengths of both the Incucyte® System and iQue® HTS Platform, researchers can obtain comprehensive and high-resolution data on various aspects of MSC biology. The ability to quantify growth dynamics, cellular morphology, senescence, and marker expression in real-time and using minimal sample volumes is particularly advantageous.

The non-destructive nature of live-cell assays ensures that valuable cell populations are preserved for further use, enhancing the efficiency and effectiveness of MSC-based research and therapies.

Furthermore, the insights gained from this integrated workflow can inform the optimization of culture conditions, passage strategies, and expansion protocols, ultimately leading to improved outcomes in MSC-based clinical applications. By ensuring that MSCs meet stringent quality criteria, researchers can enhance the reliability and efficacy of MSC-based treatments, contributing to the advancement of regenerative medicine and cell therapy.

References

1. Kurtzberg J, Prockop S, Teira P, Bittencourt H, Lewis V, Chan KW, Horn B, Yu L, Talano JA, Nemecek E, Mills CR, Chaudhury S. Allogeneic human mesenchymal stem cell therapy (remestemcel-L, Prochymal) as a rescue agent for severe refractory acute graft-versus-host disease in pediatric patients. *Biol Blood Marrow Transplant*. 2014. Vol. Feb, 20(2). 229-35.
2. Ester Moñivas Gallegoa, Mercedes Zurita Castillo. Mesenchymal stem cell therapy in ischemic stroke trials. A systematic review. *Regenerative Therapy*. 2024. Vol. Dec, 27. 301-306.
3. Tan, F., Li, X., Wang, Z. et al. Clinical applications of stem cell-derived exosomes. *Signal Transduction and Targeted Therapy*. 2024. 9. 17.
4. Dominici, M., et al. Minimal criteria for defining multipotent mesenchymal stromal cells. The International Society for Cellular Therapy position statement. *Cytotherapy*. 2006. Vol. 8, 4. 315-317.
5. Zhijie Weng, Yigan Wang, Takehito Ouchi, Hanghang Liu, Xianghe Qiao, Chenzhou Wu, Zhihe Zhao, Longjiang Li, and Bo Li. Mesenchymal Stem/Stromal Cell Senescence: Hallmarks, Mechanisms, and Combating Strategies. *Stem Cells Translational Medicine*. 2022. Vol. Apr, 11(4). 356-371.

Keywords or phrases:

Mesenchymal stem cells, Differentiation,
Cell therapy, Tissue engineering, Live-cell analysis,
Osteogenesis, Adipogenesis

Rapid Assessment of MSC Differentiation with Non-Invasive Monitoring and HTS Cytometry

Authors: Natasha Lewis, Jasmine Trigg, Daryl Cole, Nicola Bevan
Sartorius UK Ltd, Royston, Hertfordshire, UK

Correspondence
Email: askascientist@sartorius.com

Abstract

Mesenchymal stem cells (MSCs) are adult stem cells with multipotent differentiation potential and significant immunomodulatory capacity, making them highly valuable in regenerative medicine, tissue engineering, and cell therapy. Ensuring the therapeutic efficacy of MSCs necessitates rigorous confirmation of their differentiation potential into specific cell types, such as osteoblasts and adipocytes. Traditional endpoint assays for assessing MSC differentiation are limited in providing dynamic insights, highlighting the need for advanced technologies that offer real-time, high-throughput, and multiparametric analysis. This study utilizes the Incucyte® Live-Cell Analysis System and iQue® High-Throughput Screening Cytometer to monitor MSC differentiation in real-time. These technologies enable continuous live-cell imaging and rapid, multiplexed analysis, offering a comprehensive view of the differentiation process. The results demonstrate quicker confirmation of differentiation potential and preservation of cellular material for further analysis, enhancing the efficiency and reliability of MSC research.

Introduction

Mesenchymal stem cells (MSCs) are adult stem cells resident predominantly in the bone marrow alongside other sites including adipose tissue, umbilical cord blood, and dental pulp. They are self-renewing and have differentiation potential to the chondrocyte, osteocyte, and adipocyte lineages. MSCs have known capacities in immunomodulation and paracrine effects that stimulate tissue repair and regeneration. Their multi-potency and functionality make them of great interest in the fields of regenerative medicine, tissue engineering, and cell therapy, both in terms of direct repair and for treating inflammatory and autoimmune diseases. As the body of research into these unique cells grows, so does their medical potential. Clinical examples of the use of MSCs include treatment of osteoarthritis,¹ graft versus host disease,² and acute myocardial infarction.³

The therapeutic efficacy of MSCs is critically dependent on their differentiation potential into specific cell types, which is a highly regulated process influenced by various biochemical and physical cues. Osteogenic differentiation leads to the formation of osteoblasts, which are essential for bone formation and remodeling. Differentiation promoting factors elicit the expression of osteogenic markers including alkaline phosphatase (ALPL) and extracellular deposition of calcium phosphate (hydroxyapatite). Adipogenesis leads to the formation of adipocytes which play a vital role in tissue homeostasis by storing energy as fat. As such, key features of adipocytes include characteristic cytoplasmic lipid droplets, a rounded morphology, and expression of adipogenic markers and adipokines.

The ability of MSCs to differentiate must be rigorously confirmed before they can be utilized in downstream applications, as it is a key characteristic used for their identification.⁴ Traditional methods for assessing MSC differentiation are often endpoint assays, which provide limited insights into the dynamic processes of differentiation. This limitation underscores the need for advanced technologies that can offer real-time, high-throughput, and multiparametric analysis.

Addressing these challenges requires the development and adoption of standardized, reliable, and reproducible methods for MSC differentiation assessment, using advanced technologies such as the Incucyte® Live-Cell Analysis System (Incucyte® System) and iQue® High-Throughput Screening (HTS) Cytometer. Continuous live-cell imaging allows researchers to monitor morphological changes and differentiation markers over time. This method provides valuable insights into the kinetics of cell differentiation, proliferation, and morphology, offering a dynamic view of cellular processes that static endpoint assays cannot capture. Meanwhile, HTS by cytometry facilitates rapid, multiplexed analysis of cellular phenotypes and secreted factors, providing a comprehensive view of the differentiation process. The iQue® platform's high-throughput capabilities allow for the simultaneous analysis of multiple parameters across large sample sets, significantly enhancing the efficiency and depth of MSC research.

Here, we present a comprehensive workflow to evaluate the functionality of MSCs. This workflow aims to provide robust and reliable methods for assessing MSC differentiation, thereby enhancing the reliability and efficiency of experimental workflows and ensuring the therapeutic potential of MSCs is fully realized.

Materials and Methods

Media for Routine Cell Culture and for Differentiation

Materials	Supplier	Cat. No.	Final Concentration
MSC NutriStem® XF Medium	Sartorius	05-200-1A	
MSC NutriStem® XF Supplement Mix	Sartorius	05-201-1U	
MSCgo™ Osteogenic Differentiation Medium	Sartorius	05-440-1B	
MSCgo™ Rapid Osteogenic Differentiation Medium	Sartorius	05-442-1B	
MSCgo™ Adipogenic SF, XF Supplement Mix I	Sartorius	05-331-1-01	
MSCgo™ Adipogenic SF, XF Supplement Mix II	Sartorius	05-332-1-15	
NutriCoat™ Attachment Solution	Sartorius	05-760-1-15	1:500
Incucyte® Opti-Green Reagent (supplied with Incucyte® Mouse IgG1 Fabfluor Antibody Labeling Dye)	Sartorius	4745	0.5 µM
Calcein	Merck	CO875	1 µM
BioTracker 488 Green Lipid Droplet Dye	Merck	SCT144	1:1,000
Bone marrow mesenchymal stem cells RoosterVial™-hBM	RoosterBio	MSC-003	

Table 1: Cell culture media and reagents used for culturing MSCs.

Surface Marker Expression Panel Reagents

	Marker	Product Name	Supplier	Cat. No.	Final Concentration
Viability		Zombie Violet™ Fixable Viability Kit	BioLegend	423113	1:200
MSC marker panel	CD34	FITC anti-human CD34 Antibody	Invitrogen	MA5-16925	1:100
	CD45	Brilliant Violet 570™ anti-human CD45 Antibody	BioLegend	304033	1:100
	CD73	APC anti-human CD73 (Ecto-5'-nucleotidase) Antibody	BioLegend	344005	1:100
	CD90	PE/Dazzle™ 594 anti-human CD90 (Thy1) Antibody	BioLegend	328133	1:100
	CD105	PE/Cyanine7 anti-human CD105 Antibody	BioLegend	323217	1:100
Fixative		Fixation buffer	BioLegend	420801	1X
Permeabilization buffer		Intracellular Staining Perm Wash Buffer (10X)	BioLegend	421002	1X
Osteogenesis marker	Alkaline phosphatase (ALPL)	Human Alkaline Phosphatase/ALPL PE-conjugated Antibody	R&D Systems	FAB1448P-025	1:100
Adipogenesis marker	Fatty Acid Binding Protein 4 (FABP4)	Alexa Fluor® 647 Anti-FABP4 antibody	Abcam	ab216529	1:100

Table 2: Reagents used for cell analysis using the iQue® Cytometer.

MSC Culture

Prior to seeding into culture vessels for routine culture and experiments, plates and flasks were pre-coated with NutriCoat™ Attachment Solution. The solution was diluted in PBS according to the recommended volumes, added to the culture vessel and incubated for 1 hour in a humidified CO₂ incubator (37°C). Prior to cell seeding, the solution was aspirated, and cell culture medium containing a cell suspension was quickly added to ensure that the coating did not dry out.

MSCs were obtained from RoosterBio and cultured in MSC Nutristem® XF basal medium (basal medium). They were seeded at a density of 3,000 cells/cm² in tissue culture flasks, passaged at 80% confluency and analyzed using the Incucyte® System.

MSC Differentiation

MSCs were differentiated into osteoblasts using either MSCgo™ Osteogenic Differentiation Medium or MSCgo™ Rapid Osteogenic Differentiation Medium. Briefly, MSCs were seeded into 24-well plates pre-coated with MSC attachment solution at 6×10^4 cells/well (3×10^4 /cm²) in basal medium. After 24 hours, or when the cells had reached 80% confluency, the medium was exchanged to differentiation medium containing Incucyte® Opti-Green (background suppressor) and calcein. Cells were cultured in differentiation medium for either 21 or 10 days, respectively.

MSCs were differentiated into adipocytes using MSCgo™ Adipogenic Differentiation Medium. Briefly, MSCs were seeded into 24-well plate pre-coated with MSC attachment solution at 6×10^4 cells/well (3×10^4 /cm²) in basal medium. After 24 hours or when the cells had reached 80% confluency, the medium was exchanged to differentiation medium containing Incucyte® Opti-Green and BioTracker 488 Green Lipid Droplet Dye. Following 12 days of culture, the medium was exchanged to complete basal medium, and the cells were cultured for a further 4 days.

Throughout differentiation, high-definition phase-contrast and green fluorescence images were acquired using the Incucyte® System and analyzed using integrated software. Label-free quantification was performed using the Incucyte® AI Cell Health Analysis Software Module, which enables AI-based segmentation of heterogeneous cell morphologies to give univariate morphology metrics (AI Cell Segmentation),

Surface Marker Expression

At regular time points throughout differentiation, cells were stained for viability and with the MSC marker panel (CD34, CD45, CD73, CD90, and CD105) as well as specific lineage

differentiation markers. Briefly, following harvest using trypsin, cells were washed in PBS and stained for viability using Zombie Violet™ for 20 minutes. The cells were seeded into a 96-well V-bottom plate at 20K/well and washed twice with PBS + 2% FBS before staining with the MSC marker antibody cocktail as described in Table 2 for 30 minutes at room temperature. The cells were washed twice by centrifugation (5 min at 1,000 × g) using PBS + 2% FBS. Cells were then resuspended in 20 µl of PBS + 2% FBS and analyzed on the iQue® HTS cytometer.

For ALPL, a surface marker, live cells were stained with the ALPL antibody in parallel to the marker panel. For intracellular Fatty Acid Binding Protein 4 (FABP4) staining, cells were fixed using fixation buffer for 20 minutes at room temperature, washed twice in permeabilization buffer, and then stained with FABP4 antibody in PBS + 2% FBS for 30 minutes at room temperature. Cells were washed twice by centrifugation before being analyzed using the iQue® Platform. Data was analyzed using integrated iQue Forecyt® Software.

Results

Real-Time Quantification of Osteogenic Differentiation

A key indicator of MSC quality is the ability to differentiate into cells of multiple lineages, including osteoblasts. Osteogenic differentiation is typically evaluated using an endpoint histological stain for mineralized calcium deposits such as Von Kossa or Alizarin Red S staining. However, these differentiation experiments can typically last for 21 days before the differentiation can be confirmed, the staining process can be time consuming and labour-intensive, they require destruction of the cell samples, and they are typically only semi-quantitative without further laborious analysis steps. A live-cell solution would allow quicker confirmation of the differentiation potential, insight into the dynamics of the differentiation process, and preservation of precious cellular material for further evaluation including surface marker analysis.

Here, we demonstrate a simple assay for live-cell quantification of osteogenic differentiation in real-time. Calcein (not to be confused with the viability stain calcein AM) binds to the calcium in growing calcium phosphate and calcium carbonate crystals, which are extracellularly deposited as cells are directed to the bone lineage. As calcein can be incubated with cells for the duration of an experiment, it can be used for continuous assessment of mineralization, and in 3D cultures has been used as a superior alternative to Alizarin Red.⁵

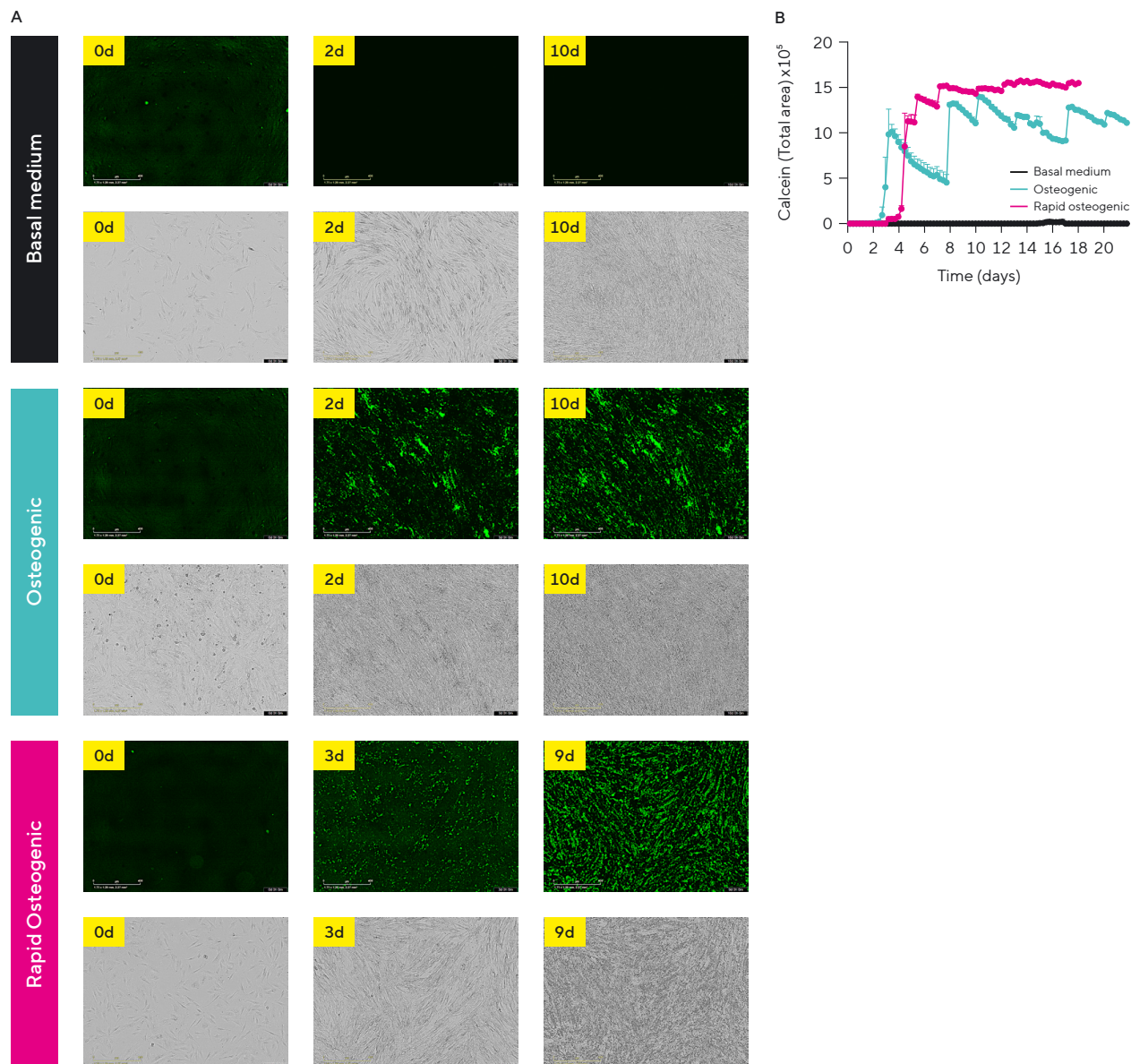


Figure 1: Fluorescent Evaluation of Osteogenic Differentiation of MSCs Cultured in Osteogenic Differentiation Medium Using Live-Cell Analysis. (A) Representative fluorescence and phase-contrast images of MSCs cultured in osteogenic medium, rapid osteogenic medium or MSC basal medium with calcein at intervals during a 21-day period. (B) Quantification of fluorescent calcein signal from images captured during the differentiation period.

Figure 1A demonstrates that osteogenic differentiation can be fluorescently detected as early as 2 days, as indicated by the appearance of green fluorescent deposits within the culture at that time point. In contrast, no fluorescent signal was observed in the control condition. There was also a visual difference in the morphology of cells cultured in osteogenic medium compared to those in basal medium, although it was more subtle and the mineral deposits were only distinct at the later time points. Thus, the calcein stain allows a robust, non-perturbing and clear early detection method for evaluating osteogenic differentiation.

Rapid osteogenic medium offers faster differentiation of osteoblasts, with a differentiation timescale of 15 days rather than 21 days. Similar to the osteogenic medium, calcium fluorescence was observable in cells cultured in the rapid differentiation medium 3 days post-culture initiation (Figure 1A). The mineral deposition was visible by eye after 6 days, and the pattern of deposition was slightly more regular than in the osteogenic medium.

Figure 1B depicts the quantification of this fluorescent signal throughout the differentiation period. In cells cultured in osteogenic media, there was an evident increase in the total fluorescent area beginning at 48 hours post-culture initiation, rapidly reaching a plateau which was broadly maintained for the remaining experimental time course. The peaks and slow decreases in the fluorescent signal reflect the replenishment of the calcein dye during media changes followed by a small amount of bleaching due to the fluorescent imaging. Differentiation as indicated by calcein fluorescence could also be easily quantified for cells in rapid osteogenic medium, with a significant rise following the change to rapid osteogenic medium, reaching a plateau that was maintained for the remainder of the experiment, with less variation arising from media replenishment.

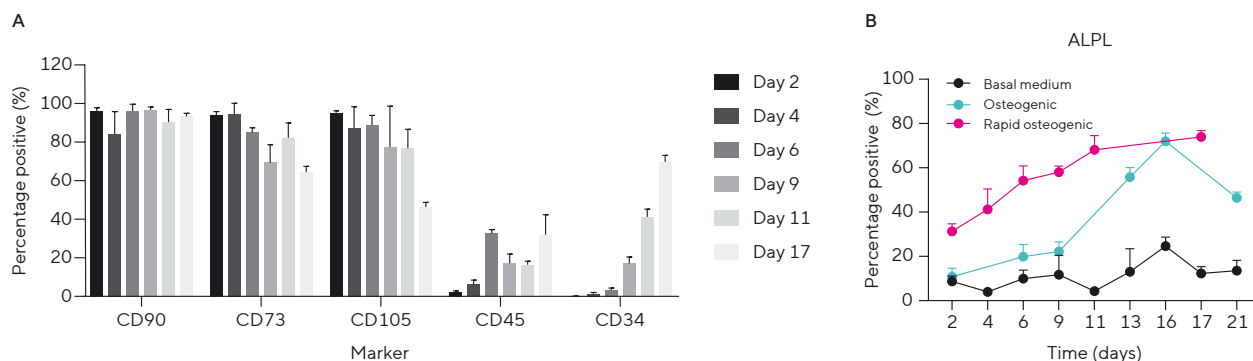


Figure 2: Expression of MSC and Osteogenic Differentiation Markers During Culture With Osteogenic Differentiation Medium as Evaluated Using HTS by Cytometry. (A) Expression of markers of MSC identity when MSCs are cultured in rapid osteogenic medium. (B) Quantification of alkaline phosphatase (ALPL) expression as an indicator of osteogenic differentiation.

Osteogenic differentiation can also be confirmed and quantified by investigating cellular identity using cell surface marker expression. MSC identity, representing a multipotent, self-renewing population, is typically defined as positive expression of CD90, CD73, and CD105, and lack of expression of CD45 and CD34. Figure 2 shows the changes in cellular marker expression during the differentiation period using rapid osteogenic media. The decreases in positive markers and increase in negative markers indicate a reduction in the self-renewing MSC population as the differentiation progressed.

ALPL is expressed at a low level in undifferentiated MSCs. However, during the experiment there was a clear increase of ALPL in the cells cultured in osteogenic medium and rapid osteogenic medium compared to basal medium, indicating that the cells were directed to the desired osteoblastic cellular identity (Figure 2B). In rapid osteogenic medium, ALPL expression was markedly increased above the control, rising from around 25% positive at day 2 to around 70% at day 17, indicating a substantial population of maturing

osteoblasts. ALPL is primarily expressed by osteoblasts during the early stages of osteogenic differentiation and bone formation. It is a marker of osteoblast activity and is involved in the mineralization process. The reduction in ALPL towards the end of the experiment with osteogenic medium may be indicative of the osteoblast maturation into osteocytes, which arise once osteoblasts are surrounded by their own matrix. Once mature osteocytes become embedded in the bone matrix, the expression of ALPL significantly decreases.⁶

Real-Time Quantification of Adipogenic Differentiation

Adipogenic differentiation, similarly to osteogenic, is usually detected using a destructive, endpoint histological stain such as Oil Red O. These methods are semi-quantitative, have low sensitivity for early differentiation, and are labor intensive. A live-cell analysis approach is a desirable alternative with obvious benefits. Here, a fluorescent lipid dye was employed for the early detection of adipogenesis through labeling of the characteristic formation of lipid droplets within the cells.

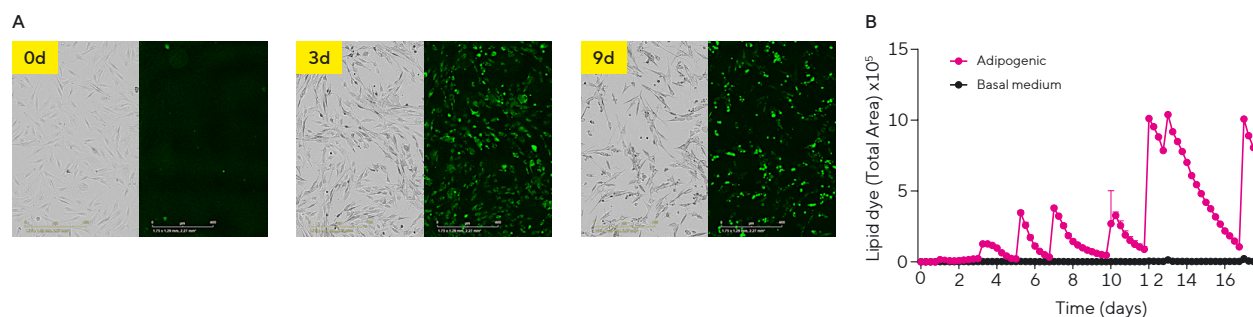


Figure 3: Fluorescent Evaluation of Adipogenic Differentiation of MSCs Cultured in Adipogenic Differentiation Medium Using Live-Cell Analysis. (A) Representative fluorescence and phase-contrast images of MSCs cultured either in adipogenic medium or basal medium with fluorescent lipid dye, acquired at intervals during a 15-day period. (B) Quantification of fluorescent lipid signal from images acquired during the differentiation period.

The formation of lipid droplets within the differentiating MSCs is distinctly visible in the images in Figure 3A. The green fluorescent signal was detectable by day 3 following culture initiation in the cells cultured with adipogenic medium, with very low staining in the control basal medium MSCs. Adipocyte morphology with internal lipid droplets can be observed in the phase images, co-localized to the droplet stains. The quantification of the lipid signal is presented in

Figure 5B. For the duration of the experiment lipid staining in basal medium was negligible, in marked contrast to the adipogenic media samples, which showed a larger total fluorescent area from day 3 following the start of the differentiation process. The peaks and slow decreases in fluorescent staining here correspond to the replenishment and bleaching of the stain, similar to the calcein.

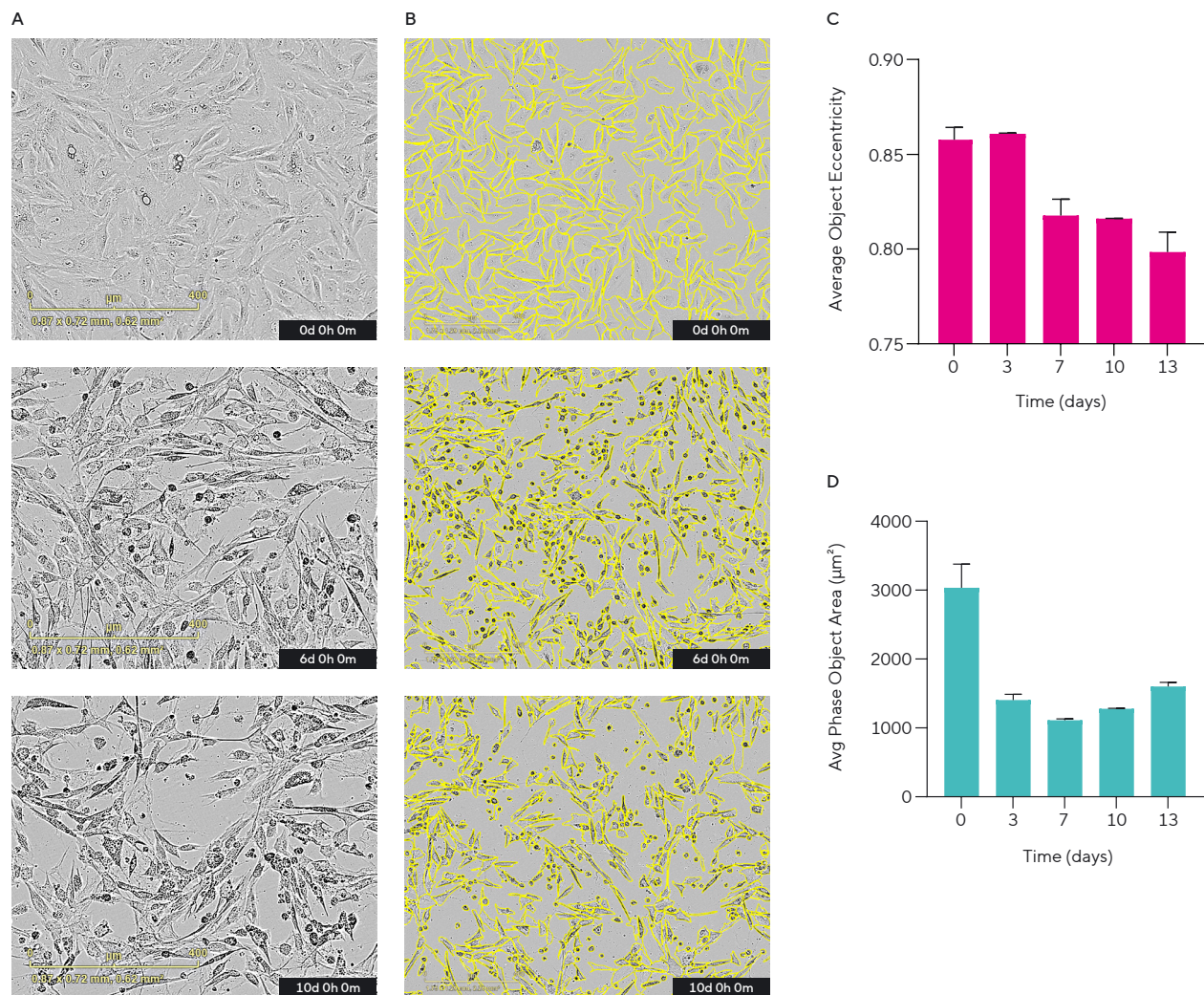


Figure 4: Analysis of Morphological Changes Accompanying Adipogenic Differentiation of MSCs Cultured in Adipogenic Differentiation Medium Using Live-Cell Analysis. (A) Zoomed phase-contrast images of cells during the adipogenic differentiation process. (B) Representative phase-contrast images of cells with overlaid AI Cell Segmentation mask (yellow outlines). (C) Average phase object area at different time points. (D) Average object eccentricity at different time points.

In addition to employing fluorescent labeling of lipid droplets to quantify adipocyte presence, their distinct morphology Figure 4A allows a label-free approach to quantifying adipogenesis. Figure 4 depicts how AI-based cell segmentation can be used to evaluate key cell metrics such as area and eccentricity on a population level and is able to accurately segment low-contrast cells with heterogenous morphologies until confluency is reached (Figure 4B). As adipogenic differentiation progresses, cell morphology

changes from flattened, spindle-shaped cells to a greater proportion of the cell population having a rounded or oval shape. This is reflected in Figure 4C and D, with both area and eccentricity initially high and decreasing as the time course progresses. These two metrics, in combination with visual assessment of the images, can be used to confirm adipogenic differentiation without requiring the addition of fluorescent reagents.

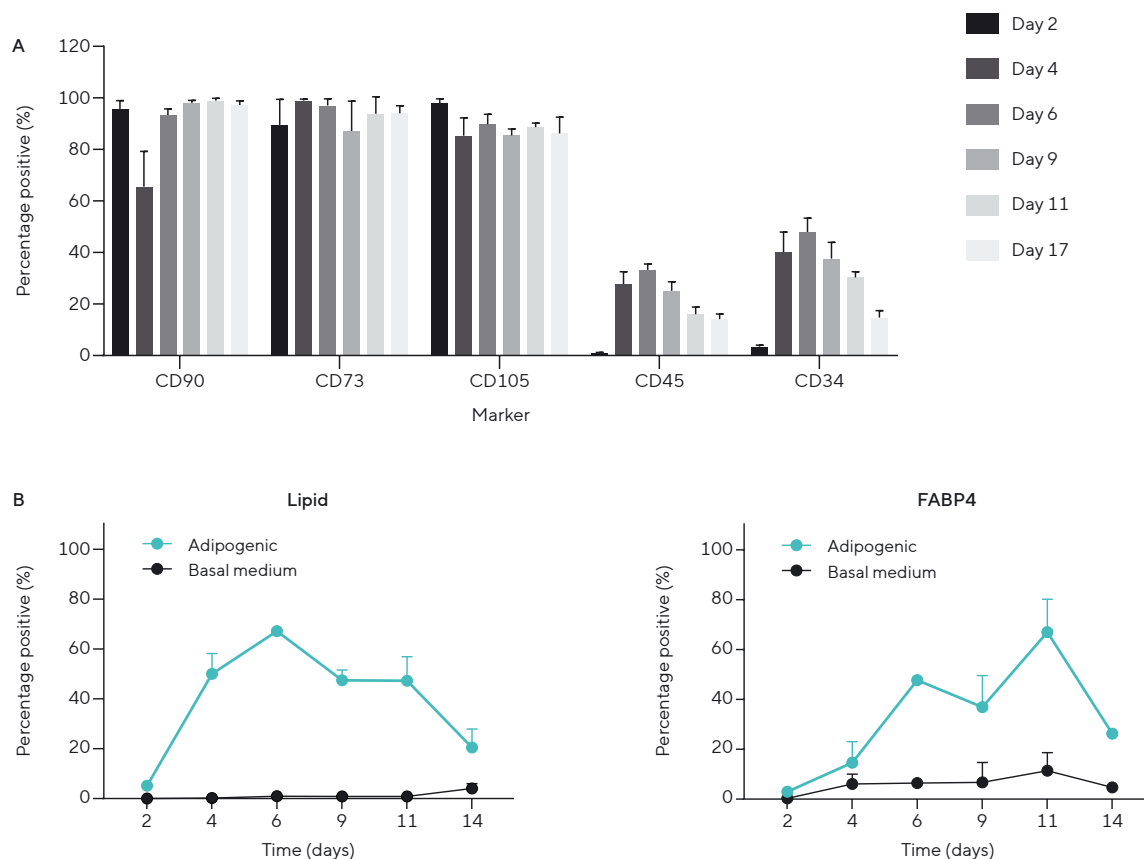


Figure 5: Expression of MSC and Adipogenic Differentiation Markers During Culture With Adipogenic Medium as Evaluated Using HTS by Cytometry. (A) Expression of markers of MSC identity. (B) Quantification of fluorescent lipid dye and FABP4 as indicators of adipogenic differentiation.

When examining expression of markers during adipogenic differentiation, a distinct change in cellular identity was observed during the process (Figure 5). As in the osteogenic differentiation, expression of positive MSC markers remained high for the duration of the experiment. However, both negative markers, CD34 and CD45, were elevated from 4 days and higher levels were maintained until the adipocytes became more mature.

The intracellular lipid dye can be detected using single cell cytometry in addition to fluorescence imaging. By day 4 of the process, 50% of the cells contained the dye, compared to 0% in the basal medium control, which is a clear early confirmation of adipogenesis. Concurrently, FABP4 expression was elevated in the adipogenic medium from day 4 of the differentiation process.

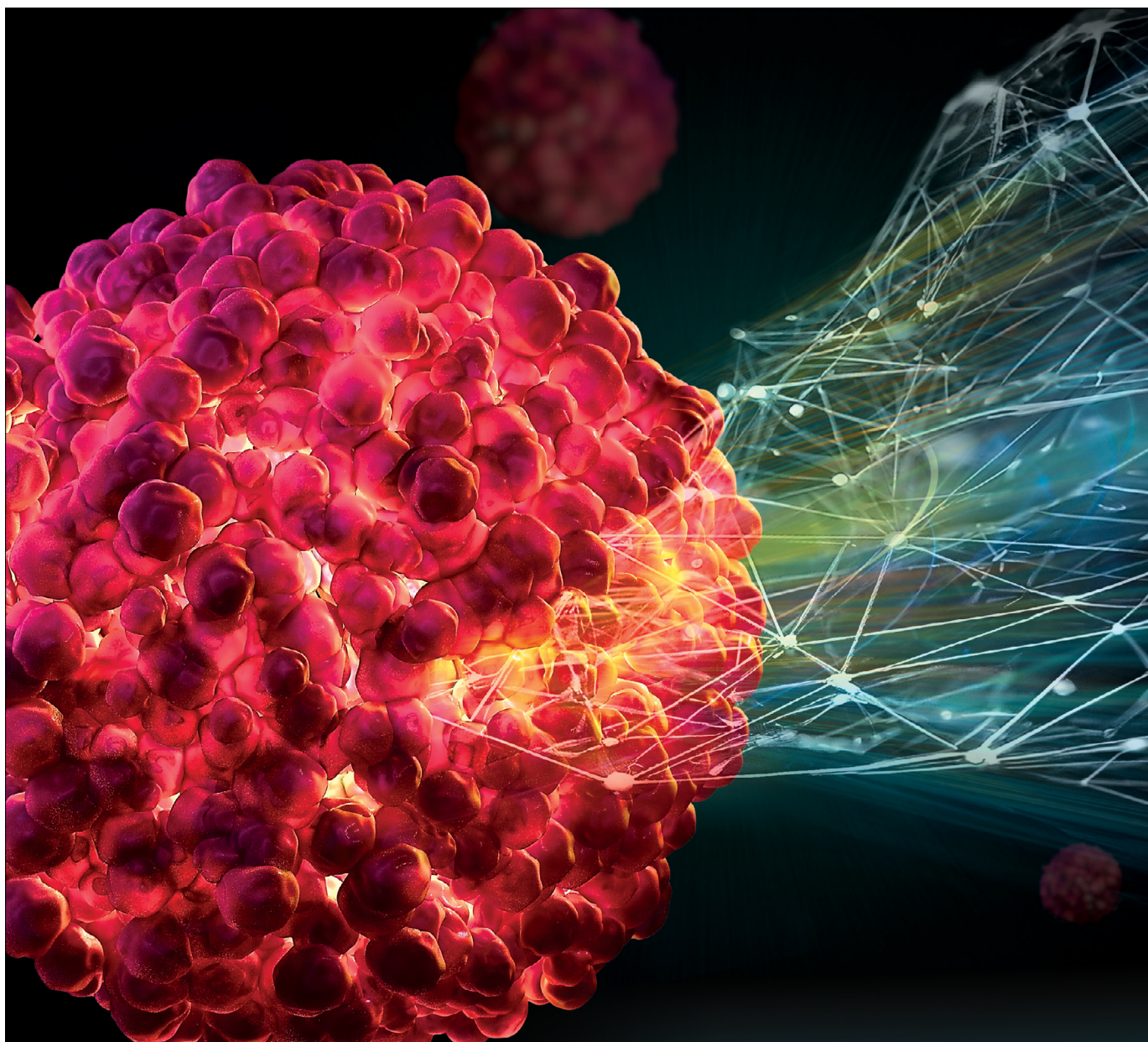
Summary and Outlook

The use of advanced analysis technologies has significantly enhanced the ability to assess MSC differentiation in real-time, providing valuable insights into the dynamics of the differentiation process. The successful application of these technologies in both osteogenic and adipogenic differentiation demonstrates their versatility and effectiveness. By providing a comprehensive view of the cellular changes, these methods pave the way for more standardized, reliable, and reproducible assessments of MSC functionality. These methods offer several advantages over traditional endpoint assays, including quicker confirmation of differentiation potential, preservation of cellular material for further analysis, and the ability to monitor multiple parameters simultaneously.

By adopting these advanced technologies, researchers can improve the efficiency and depth of MSC research, ultimately enhancing the therapeutic potential of MSCs for treating various diseases and conditions.


References

1. Lee, D.H., Kim, S.J and Kim, S.A. et al. Past, present, and future of cartilage restoration: from localized defect to arthritis. *Knee Surgery & Related Research*. 2022. Vol. 34, 1.
2. Kurtzberg J, Prockop S, Teira P, Bittencourt H, Lewis V, Chan KW, Horn B, Yu L, Talano JA, Nemecek E, Mills CR, Chaudhury S. Allogeneic human mesenchymal stem cell therapy (remestemcel-L, Prochymal) as a rescue agent for severe refractory acute graft-versus-host disease in pediatric patients. *Biol Blood Marrow Transplant*. 2014. Vol. Feb, 20(2). 229-35.
3. Yoshihisa Yamada, Shingo Minatoguchi, Hiromitsu Kanamori, Atsushi Mikami, Hiroyuki Okura, Mari Dezawa, Shinya Minatoguchi. Stem cell therapy for acute myocardial infarction – focusing on the comparison between Muse cells and mesenchymal stem cells. *Journal of Cardiology*. 2022. Vol. 80, 1. 80-87.
4. Dominici, M., et al. Minimal criteria for defining multipotent mesenchymal stromal cells. The International Society for Cellular Therapy position statement. *Cytotherapy*. 2006. Vol. 8, 4. 315-317.
5. White, Kristopher, et al. Calcein Binding to Assess Mineralization in Hydrogel Microspheres. *Polymers*. Basel: s.n., 2021. Vol. Jul 11, 13(14). 2274.
6. Franz-Odenaal, Tamara A, Hall, Brian K and Witten, P Eckhard. Buried alive: How osteoblasts become osteocytes. *Developmental Dynamics*. 2006. Vol. Jan 235, 1. 176-90.



Reproducible and Scalable Data to Maximize Organoid Research

Effective analysis of 3D cell models can be challenging. The Incucyte® Live-cell Analysis System is a turnkey solution that automatically monitors and quantifies cell formation, growth, and health in real time directly inside the incubator. Multiple assays are available for real-time visualization and label-free objective quantification to optimize organoid and spheroid culture conditions.

 www.sartorius.com/incucyte

Specifications subject to change without notice. © 2024. All rights reserved. Incucyte and all names of Sartorius products are registered trademarks and the property of Sartorius AG.

Simplifying Progress

SARTORIUS

Keywords or phrases:

Extracellular vesicles, EV labeling kit, EV uptake, EV internalization, Exosome, Exosome labeling

Harnessing Exosomes for Biomedical Applications: Insights into Extracellular Vesicle Labeling and Cellular Uptake Using Live-Cell Analysis

Author: Laura Skerlos¹, Susan Foltin¹, Hinnah Campwala¹, Eric Black², Aslan Dehghani², Nicola Bevan³, Cicely Schramm¹

1. Sartorius Corporation, 300 West Morgan Road, Ann Arbor, MI 48108, USA

2. Sartorius Stedim North America Inc., 565 Johnson Avenue, Bohemia, NY 11716, USA

3. Sartorius UK Ltd, Royston, Hertfordshire, UK


Correspondence

Email: askascientist@sartorius.com

Abstract

The Incucyte® Exofluor Green EV Labeling Kit represents a significant advancement in the study of extracellular vesicles (EVs), particularly exosomes, which play an important role in diagnostics and biomolecule transport. This kit facilitates the non-perturbing, real-time visualization and quantification of EV uptake in live cells, overcoming the challenge of assessing the functional quality of EVs post-purification. The Incucyte® Exofluor Green Dye covalently labels EVs, offering enhanced stability and specificity over traditional methods, and the kit includes necessary consumables for removing free dye and sterilizing the assay medium.

The kit has been validated across a range of EV purification methods and cell origins, demonstrating compatibility and effectiveness in live-cell assays. It also enables the study of EV uptake mechanisms and the functional analysis of EVs, such as their role in wound healing, as shown in the scratch wound assay using MSC-derived EVs. The Incucyte® Exofluor Green EV Labeling Kit is a valuable tool for researchers, providing a standardized approach to explore EV dynamics and functions in a live-cell context.

 For further information, visit sartorius.com/incucyte/ev-uptake

Introduction

Extracellular vesicles (EVs), particularly exosomes, have received significant attention in the field of diagnostics and therapeutics due to their role in transporting biomolecules. These lipid-bound particles, ranging from 50–1000 nm, are naturally secreted by cells into the extracellular space where they target acceptor cells (via activation or uptake).¹ Exosomes, a subclass of EVs also referred to as small EVs, are characterized by their size (40–160 nm) and endosomal origin.² EV research is still in its early phase, particularly regarding analytical characterization methods and purification process development. In addition to production yield and purity, researchers are keenly interested in understanding how production processes translate to cellular uptake of EVs, and ultimately transport of cargo.^{3,4,5}

While tools exist to assess the physical and chemical properties of EVs, assessing post-purification functional quality of the nanoparticles remains a significant challenge.^{1,6,7} The Incucyte® Exofluor Green EV Labeling Kit serves as a method for use with live-cells, for uptake analysis of small EVs extracted across a wide range of purification methods. The use of a covalently bound dye for labeling EVs offers several advantages over traditional membrane permeable staining methods, including enhanced stability and specificity of the label. This is a significant improvement over conventional EV labeling methods, as it minimizes the risk of non-specific staining and ensures that the observed fluorescence is due to EV uptake rather than extraneous factors. Additionally, the

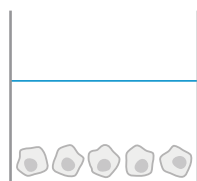
covalent labeling approach is more user-friendly and time-efficient compared to biogenesis methods of labeling EVs, which often require complex and time-consuming manipulations of the EV-producing cells. This application note demonstrates the validation and use of the Incucyte® Exofluor Green EV Labeling Kit as a new offering to the field of EV research.

Assay Principle

The Incucyte® Exofluor Green EV Labeling Kit enables non-perturbing, real-time and dynamic evaluation of cellular EV uptake and has been validated for use with the Incucyte® Live-Cell Analysis System configured with a green | red or green | orange | near-IR optical module. The specificity of staining and non-perturbing chemistry of the Incucyte® Exofluor Green Dye is favorable to use in live-cell assays over commonly used EV labeling lipophilic dyes like DiO and Dil. Incucyte® Exofluor Dye uniformly and irreversibly labels the plasma membrane of small EVs by covalently binding to proteins and amino acids. The irreversible binding to the EVs eliminates the risk of non-specific dye attachment to other plasma membranes before or during uptake. In addition to the dye, the kit contains the consumables necessary to remove free dye (Vivaspin®2 columns) and sterilize medium while removing aggregates (Minisart® 0.22 µm filters) (Figure 1).

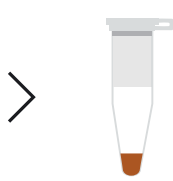
Quick Guide

1. Cell Seeding



Seed cells in growth media and leave to adhere (4–24 hours). Cells should be 15–35% confluent at the time of treatment.

2. EV Labeling



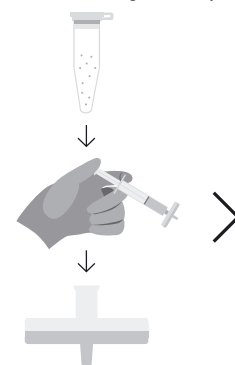
Reconstitute Incucyte® Exofluor Green EV Labeling Dye in DMSO and add to EVs at a final concentration of 80 µM. Incubate labeling reaction for 30 minutes at 37 °C.

3. Free Dye Removal



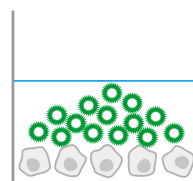
Add EV labeling reaction to the Vivaspin® 2 column (max load 40 µg or 100 µL per column) and spin at 2000 x g for 5 minutes to remove free dye.

4. Post-labeling Clean Up



Collect labeled EVs from the Vivaspin® 2 in Assay Medium and load into a syringe. Pass mix through a Minisart® filter (0.22 µm) to sterilize and remove aggregates.

5. Treatment of Cells with Labeled EVs



Perform a full media replacement with labeled EV containing media.

Figure 1: Quick Guide schematic illustrating Incucyte® Exofluor Green EV Labeling Kit method.

Methods and Materials

Cell Culture

Adherent cell lines were cultured in medium supplemented with 10% fetal bovine serum: Ham's F12 Nutrient Mix with GlutaMax™ (A549, HT1080, PC3, MDA), Dulbecco's Modified Eagle Media (NIH-3T3, NHDF), or Minimum Essential Medium (HEK293T). Cells were grown at 37°C, 5% CO₂ to about 90% confluency prior to passage. EV uptake assays using normal human dermal fibroblasts (NHDF) were performed with cells passaged no more than five times. To perform standard EV uptake assays, adherent cell lines were seeded at 15–35% confluence (1.5–3K cells/well) in 96-well microplates and allowed to adhere to plate (4–24 hours) prior to treating with EVs.

EV Labeling Protocol

Prior to the EV labeling reaction, the Incucyte® ExoFluor Dye was reconstituted to 5 mM using anhydrous DMSO and then diluted 1:10 using Phosphate Buffer Saline (PBS Ca²⁺/Mg²⁺ free). To set-up the labeling reaction, Incucyte® ExoFluor Dye (500 µM) was added directly to EV samples for a final concentration of 80 µM and incubated at 37°C for 30 minutes. The amount of EVs labeled was calculated based on the EV concentration required per well (protein or particle count depending on EV protein concentration) and the number of wells tested (n ≥ 3). The commercially available EVs contained roughly 10-times higher protein than in-house produced EVs. In this work, higher protein EVs were optimized in range of 1–4 µg of protein/well whereas lower protein EVs were optimized at 5 E7–1 E9 particles/well. The kit has been validated for use with EVs isolated using a variety of extraction methods and cell origin: precipitation (A549, PC3, human serum), ultrafiltration (A549), ultracentrifugation (MSC, human plasma), Tangential Flow Filtration (TFF)/Size Exclusion Chromatography (SEC) (A549 and U87) and TFF/ion exchange chromatography (IEX) (MSC, HEK293T) methods.

After the 30-minute incubation, the EV labeling reaction was removed from 37°C incubator, placed at room temperature, and diluted using PBS at a 2–4 X volume. To prevent the carry-over of free dye leading to non-specific fluorescent signal in the assay plate, the diluted labeling reaction was transferred to Vivaspin® 2 protein concentrator column(s) and centrifuged at room temperature (2000x g for 5 minutes). For EV samples containing a higher protein concentration, the amount of labeling reaction loaded on the Vivaspin® 2 did not exceed 40 µg protein as exceeding this limit can lead to membrane clogging. Low protein EV samples were loaded to Vivaspin® 2 columns such that the volume of the dye did not exceed 20 µL (or 100 µL EVs) as high dye volume can increase background fluorescence.

Labeled EVs were further purified on the Vivaspin® 2 with a PBS wash followed by a dry spin to ensure removal of all free dye. Labeled EVs were recovered off the Vivaspin® 2 by adding warmed assay medium (base medium supplemented with exosome-depleted FBS, Thermo Cat. No. A2720801) and pipetting up-and-down several times. Using a P200 gel loading tip (PR1MA Cat. No. PR-200XLRK-FL), medium-containing labeled EVs was collected off the Vivaspin® 2 column and transferred to a fresh tube. EVs were loaded into a syringe, using a blunt end tip (Stemcell Cat. No. 28110), in preparation for final sterilization and removal of unbound aggregates. The blunt end tip on the syringe was replaced with a Minisart® 0.22 µm syringe filter and EVs were pushed slowly through the filter into a fresh collection tube.

On the day of assay, growth medium was carefully removed from the cell plate and labeled EVs were added to appropriate wells on the plate. Imaging of both HD phase-contrast and green fluorescence channels using the 10X objective was performed every 30 to 60 minutes on an Incucyte® Live-Cell Analysis System, and results were quantified using the Incucyte® Adherent Cell-by-Cell (CBC) Analysis Software Module.

Scratch Wound Assay

Incucyte® Imagelock 96-well Plates (Cat. No. BA-04855) were coated with 50 µL per well Collagen I, rat tail (100 µg/mL, Corning® Cat. No. 354236) for 2-hours at room temperature. After incubation, wells were rinsed with PBS (1X) and allowed to air dry. NHDF cells were harvested using TrypLE (Invitrogen Cat. No. 12605-010), counted, and resuspended in DMEM + 10% FBS prior to adding to the Collagen I coated plates at a seeding density of 15K cells per well. Cells were allowed to settle in the plate for 15 minutes and incubated overnight so that cells could adhere to the plate. An Incucyte® 96-Well Woundmaker Tool (Cat. No. 4563) was used according to standard protocol to create uniform wounds across the collagen coated/seeded assay plate. After wounding, media was aspirated and cells were washed 2X with 100 µL of assay medium (serum free DMEM). After rinse, 100 µL of fresh assay medium, with or without EVs was added to assay plate. The plate was analyzed in an Incucyte® Live-Cell Analysis System using the Incucyte® Scratch Wound Analysis Software Module to quantify the EV-mediated wound closure.

Results

Validation of the EV Kit

More than a dozen EV sources were tested during the validation of the Incucyte® Exofluor EV Labeling Kit. Figure 2 shows representative data analysis tools using exosomes purchased from Systems Biosciences, derived from PC3 human prostate cancer cells and purified using a precipitation method (ExoQuick-TC, SBI). PC3 exosomes were characterized by the manufacturer using NanoSight (90–110 nm, ~1 E10 exosomes/mL), Western blot analysis (CD63 exosome biomarker validation), and protein concentration (50 µg). The PC3 exosomes were labeled using the Incucyte® Exofluor EV Labeling Kit and A549 uptake cells were treated at 2 and 4 µg/well. Figure 2A shows the Average Green Object Mean Intensity (GCU)

measurement across wells (n=4) with labeled exosomes versus control conditions. While the fluorescence is negligible in the control conditions (Dye Only and Medium Control), an expected concentration-dependent increase in fluorescence was observed for the cells treated with labeled exosomes. Furthermore, cell proliferation measured as cell count was undisturbed across conditions (data not shown) demonstrating no effect on cell health. Using CBC analysis, a post-processing histogram was used to classify populations based on Green Mean Intensity (High vs Low). Using this classification, the High Green Intensity (% Total) population of cells was plotted to demonstrate the percentage of cells taking up the labeled EVs across the population over the course of 60 hours. (Figure 2B and 2C).

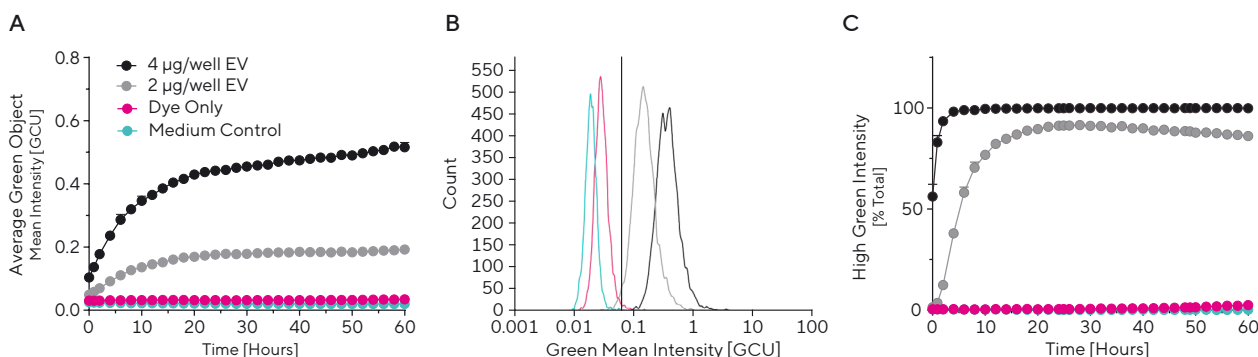


Figure 2: Data Analysis Tools to Measure Uptake of Incucyte® Exofluor Green Labeled EVs

The Average Green Object Mean Intensity increased as a measure of the A549 cells taking up labeled, PC3 EVs (A). Histogram analysis is used to classify populations of segmented cells at 24-hours (B). Quantification of the percentage of labeled cells, classified as having high green intensity, over time (mean ± SEM, n=4) (C).

In order to further validate the kit for live-cell analysis, a range of adherent uptake cell lines were studied to verify: (1) uptake of labeled EVs is non-perturbing, (2) fluorescent signal can be measured across different growth mediums, and (3) fluorescent signal is not due to unlabeled dye. This analysis was carried out using lyophilized exosomes purified from conditioned A549 medium (TFF and SEC methods of purification) and characterized (NTA, Zetaview, Western blot, FACS, and RT-PCR) by HansaBioMed. Figure 3A shows images from PC3, HEK293T, and NIH-3T3 cells treated with labeled A549 exosomes (2 µg per well) or Dye Alone. CBC data for Labeled EV wells (n=4) were analyzed alongside control conditions, Dye Only and Medium Control (image is not shown).

With respect to perturbation, no change in growth kinetics (quantified using Phase Count Per Image) was observed across all cell types (representative data shown in Figure 3B). Visual inspection of HD phase-contrast images corroborates processing analysis as cell morphology appears unaffected by uptake of labeled EVs. Collated data from this study also confirmed green fluorescence signal was observable and quantifiable across all conditions tested. Furthermore, image analysis also confirmed the absence of dye aggregates or exceptionally high background due to free dye.

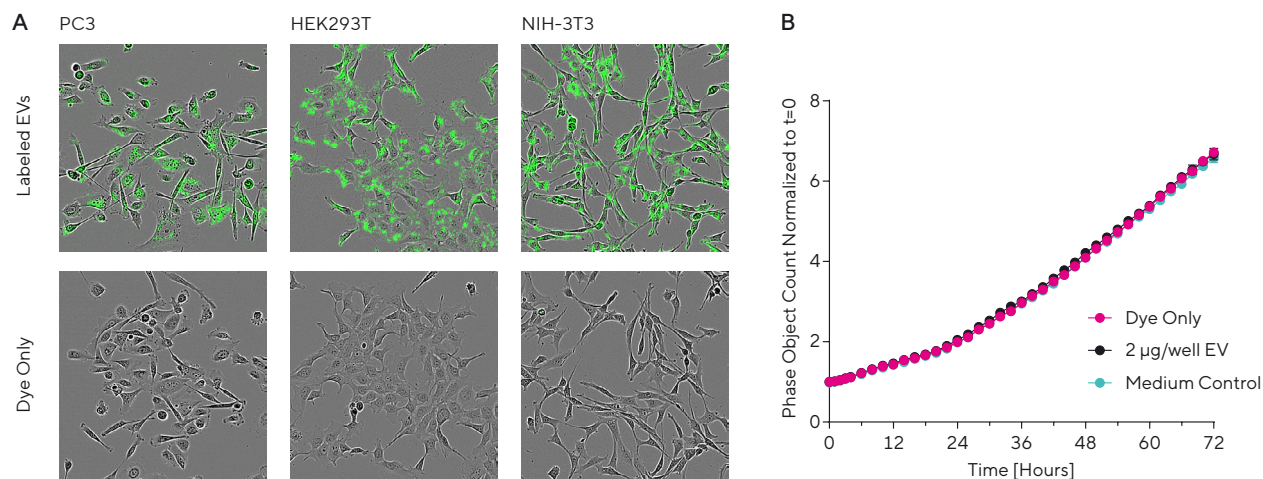


Figure 3: Uptake Cell Compatibility

A549 Exosomes (HansaBioMed) were labeled using the Incucyte® ExoFluor Dye and cell lines were treated with labeled exosomes (A, top row). Dye only control wells for each condition demonstrate the fluorescent signal is not due to residual free dye after processing (A, bottom row). Images taken at 24-hours post-treatment with labeled A549-derived exosomes across various cell types also show no change in cell morphology compared to controls. Phase Object Count normalized to t=0 (mean \pm SEM, n=4) data illustrates no change in proliferation of PC3 cells across all conditions (B).

The physical and chemical properties of an EV sample are highly dependent on the production process used to isolate the nanoparticles.⁸ Over the course of validating the EV labeling kit for use in live-cell assays, EVs representing a range of extraction and purification methods were tested. Figure 4 shows representative fluorescent images of A549 cells treated with EVs of various purity, labeled using the Incucyte® ExoFluor Dye. Exosomes derived from human plasma (lyophilized) and the A549 HansaBioMed exosomes (previously described) are two types of EVs extracted using characteristically lower purity methods. The hPlasma exosomes (purified by ultracentrifugation and microfiltration) were purchased and characterized by Abcam (NTA, FACS, Western blot, CD9/CD63 biomarker). Inversely, two EV samples prepared in-house for these studies were used as representative higher purity samples. These EVs were derived from large production batch volumes using

TFF and ion exchange chromatography methods and characterized by NTA, Virus Counter, Western blot, and SEC Chromatography. In-house EVs, derived from both MSC and HEK293T cells, contained about 10-fold less protein than both hPlasma and A549 samples. With lower protein containing EV samples (i.e. higher purity), there is less risk to overloading the Vivaspın® 2 membrane during free dye removal. For low protein EVs, particle count is used to set up labeling reaction and treatment conditions instead of protein concentration. Figure 5 illustrates a non-perturbing, concentration-dependent increase in fluorescence (GCU) for A549 cells treated with labeled high purity EVs. Taking the data from these four EV samples, along with the range of extraction methods represented throughout testing, the EV labeling kit was found to be compatible across all methods of purification.

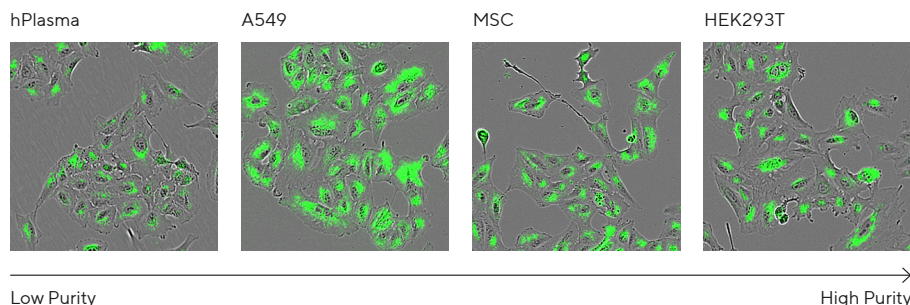


Figure 4: EV Labeling Compatibility

Images demonstrate uptake of various EVs labeled with Incucyte® Exofluor Green by A549 cells (24 hours post-treatment). Human plasma-derived exosomes (Abcam, ultrafiltration) and A549 exosomes (HansaBioMed, ultrafiltration and SEC) were labeled and added to cells at 4 and 2 $\mu\text{g}/\text{well}$, respectively. Both MSC and HEK293T EVs were extracted in-house using TFF/ion exchange chromatography and treated at 1.5 E8 and 8.3 E7 particles/well, respectively.

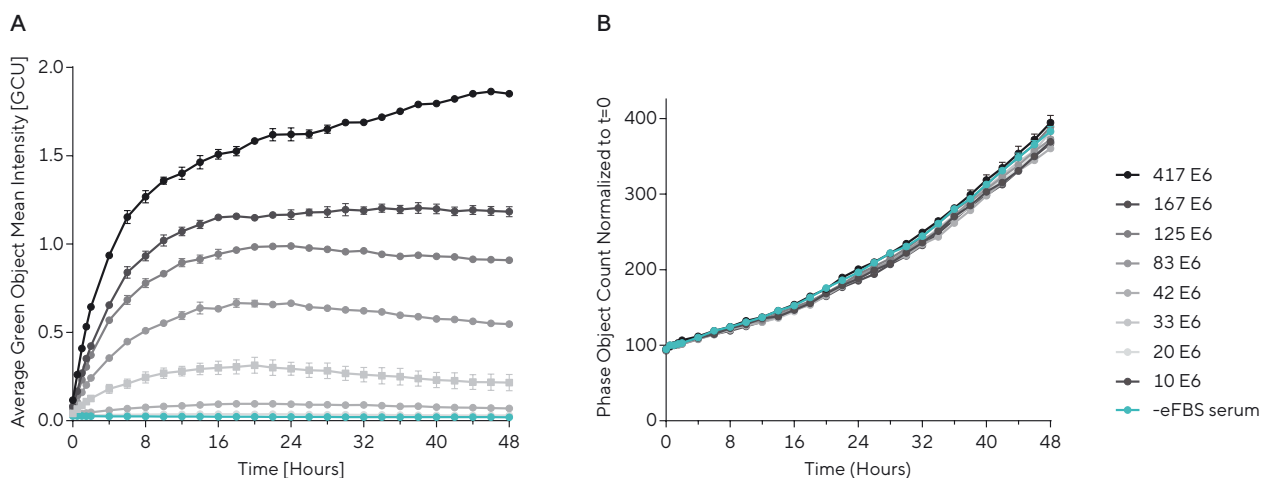


Figure 5: EV Concentration Dependence

Labeled EVs were purified from HEK293T cells in-house and titrated ~40-fold (4.17 E8 to 1 E7 particles/well). HD phase and green fluorescent images were acquired every 2 hours over the course of 48 hours and uptake was assessed using Average Green Mean Intensity (A). Phase Object Count (normalized to $t=0$) data illustrates no change in proliferation at all concentrations of EVs tested (B). Data represent mean \pm SEM ($n=3$).

Mechanism of Action

It is widely accepted that EVs are taken up by cells through one or more endocytic methods: clathrin-dependent, caveolin-dependent, phagocytosis, membrane fusion, or micropinocytosis.²⁻⁹ Dynasore is a known GTPase activity inhibitor which prevents EV uptake via clathrin-mediated endocytosis.^{9, 10} In order to further qualify this EV labeling method, the ability of Dynasore to lower the fluorescent signal (inhibit uptake of labeled EVs) was tested (Figure 6). A549 cells were seeded overnight and then treated with the endocytosis inhibitor Dynasore (0.11 to 27 μM) in exosome-

free culture medium (50 μL). Within the first 30 minutes following Dynasore treatment, assay medium containing A549 exosomes (HansaBioMed Life Sciences) labeled with Incucyte® Exofluor Green Dye (50 μL , 2 $\mu\text{g}/\text{well}$) were added to assay plate and Green Object Mean Intensity was measured. A concentration-dependent decrease in Green Object Mean Intensity was observed upon Dynasore treatment, consistent with the expected inhibition of EV uptake ($\text{IC}_{50} = 2.72 \mu\text{M}$).^{11, 12} These data corroborate the fluorescent signal is specific to the uptake of labeled EVs as opposed to non-specific, cross-labeling.

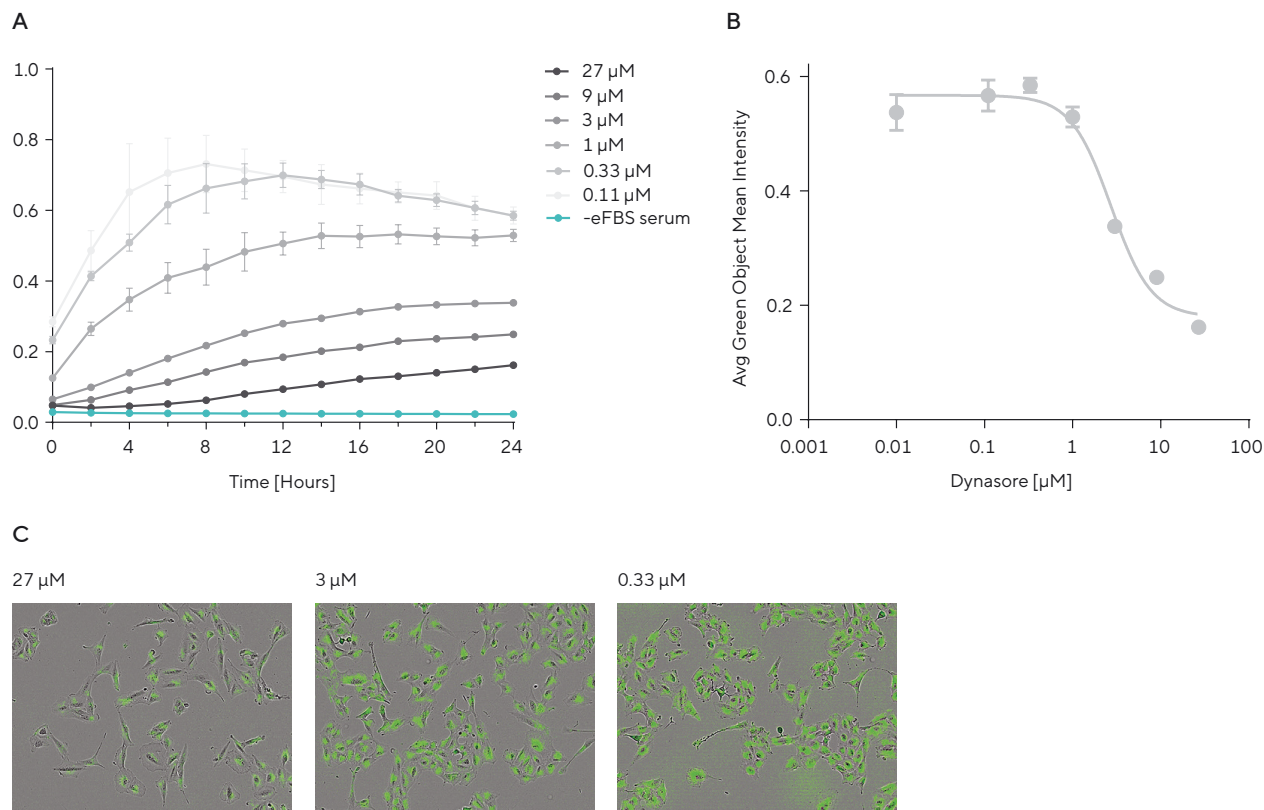


Figure 6: EV Uptake Depends on Endocytosis

Concentration-dependent inhibition of EV uptake by Dynasore in A549 cells was evaluated by measuring Green Object Mean Intensity (\pm SEM, $n=3$) over 24 hours (A). A concentration-response curve generated from 24-hour timepoint data reflected an expected drop in Green Object Mean Intensity ($IC_{50} = 2.72 \mu$ M) (B). Representative images from the same timepoint provide visualization of Dynasore inhibition of EV uptake at the indicated concentrations (C).

Scratch Wound Assay

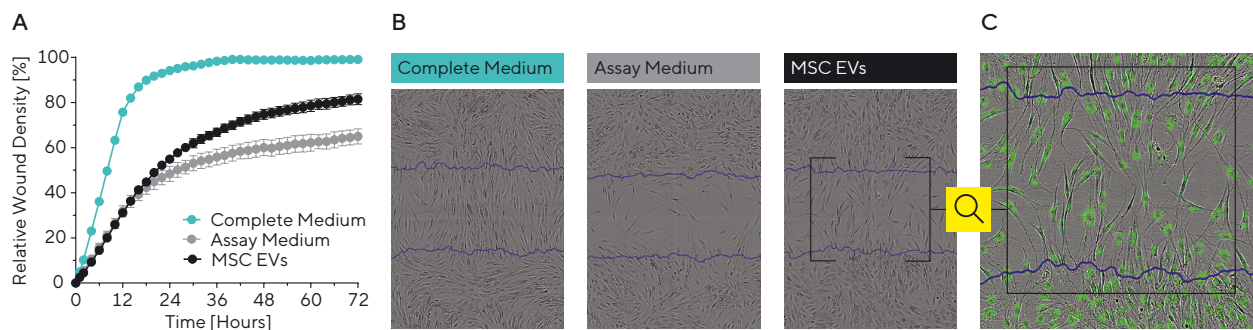


Figure 7: MSC-EVs Promote Wound Healing

NHDF Cells were seeded at 15K cells/well on collagen-coated plates, scratched, and media was replaced with Assay Medium containing MSC-derived EVs (4.5 E9 particles/well). Cell migration was captured using an Incucyte® Live-Cell Analysis System and Relative Wound Density (mean \pm SEM, $n=6$) was quantified over time (A). HD Phase images showed varying degrees of cell migration into the initial wound (blue) at 18-hours post scratch (B). Associated MSC EV uptake was demonstrated via the presence of green fluorescence in acceptor cells (C).

The Incucyte® Scratch Wound Assay paired with the EV Labeling Kit offers a promising avenue for functional analysis of small EVs in cell migration applications. Notably, exosomes derived from human mesenchymal stem cells (MSCs) have been reported to enhance cutaneous wound healing.^{13, 14} Figure 7 presents the functional uptake and transfer of cargo from labeled MSC-derived EVs using the Scratch Wound Assay. When labeled EVs were added to NHDF cells, there was a significant increase in Relative Wound Density (RWD) compared with wells treated with assay medium alone (81% vs 65% at 72 hours). NHDF cells grown in complete medium (DMEM + 10% FBS) achieved a RWD > 90% in the first 24-hours post-scratch (Figure 7A). HD phase-contrast image analysis at 18 hours post-scratch highlights the variation in cell migration across the treatment conditions (initial wound boundary is mapped for reference). Notably, the cell morphology in Complete Medium is comparable to cells growing in optimized assay conditions (serum free DMEM, Figure 7B). Green fluorescence imaging reveals the homogeneous uptake of Incucyte® Exofluor Green labeled EVs (Figure 7C). This therapeutic wound closure effect is attributed to the modulation of inflammation, proliferation, and matrix remodeling, processes that are mediated by the protein and microRNA cargo contained within the EVs.^{3, 15} Furthermore, these results suggest that the labeled EVs retain their functional properties post-labeling.

Conclusion

The Incucyte® Exofluor Green EV Labeling Kit provides a powerful platform for elucidating the biological functions of EVs by enabling researchers the ability to visualize and quantify EV uptake in real-time. This application note outlines the kit's versatility across a variety of cell lines, EV purification methods, and functional assays. The specificity of the Incucyte® Exofluor Green Labeling Dye ensures accurate tracking of EV uptake without the interference of non-specific dye attachment, as evidenced by the absence of free dye or dye aggregates in our imaging analyses. In conclusion, the Incucyte® Exofluor Green EV Labeling Kit is a valuable addition to the toolkit of researchers studying EVs. It offers a standardized approach to assess the functional quality of EVs post-purification and enables the exploration of EV dynamics in a live-cell context.

References

1. Bonsergent, E. et al. Quantitative characterization of extracellular vesicle uptake and content delivery within mammalian cells. *Nature Com* 12:1864 (2021).
2. Kalluri, R & LeBleu, VS. The biology, function, and biomedical applications of exosomes. *Science* vol 367, issue 6478 (7 Feb 2020)
3. Hettich, B. F. et al. Exosomes for wound healing: purification optimization and identification of bioactive components. *Adv. Sci.* 7. 2002596 (2020).
4. Akbar, A. et al. Methodologies to isolate and purify clinical grade extracellular vesicles for medical applications. *Cells.* 11, 186 (2022).
5. Clos-Sansalvador, M. et al. Commonly used methods for extracellular vesicles enrichment: implications in downstream analysis and use. *Euro J Cell Biol* 101, 151227 (2022).
6. Hartjes, T. A. et al. Extracellular vesicle quantification and characterization: common methods and emerging approaches. *Bioengineering* 6, 7 (2019).
7. Xu, R. et al. Extracellular vesicles isolation and characterization: toward clinical application. *J Clin Investig* 126, 1152-1162 (2016).
8. Lai, J. J. et al. Exosome processing and characterization approaches for research and technology development. *Adv Sci* 9, 15, 2103222 (25 May 2022).
9. Mulcahy, L. A. et al. Routes and mechanisms of extracellular vesicle uptake. *J Extracell Vesicles.* Aug 4:3 (2014).
10. Sinha, M. S. et al. Alzheimer's disease pathology propagation by exosomes containing toxic amyloid-beta oligomers. *Acta Neuropathol.* 136(1): 41-56 (2018).
11. Kim, J. H. et al. Dissecting exosome inhibitors : therapeutic insights into small-molecule chemicals against cancer. *Experi Mol Med* 54:1833-1843 (2022).
12. Macia, E. et al. Dynasore, a cell-permeable inhibitor of dynamin. *Developmental Cell.* 10, 839-850 (2006).
13. Zhao H. et al. Bioengineered MSC-derived exosomes in skin wound repair and regenerations. *Front Cell Dev Biol.* 11:1029671 (2023).
14. Li, C. et al. Adipose mesenchymal stem cell-derived exosomes promote wound healing through the WNT/ β -catenin signaling pathway in dermal fibroblasts. *Stem Cell Rev Reports.* 18:2059-2073 (2022).
15. Vu, N. B. et al. Stem cell-derived exosomes for wound healing: current status and promising directions. *Minerva Med.* 112 (3), 384-400 (2021).

Keywords or phrases:

Exosomes, extracellular vesicles (EVs), immuno-affinity chromatography, syringe filtration, nanoparticle tracking analysis (NTA)

Combining Immuno-Affinity Chromatography and Filtration to Improve Specificity and Size Distribution of Exosome-Containing EV Populations

Jan-Dirk Wehland¹, Fabian Mohr¹, Wiktoria Banczyk², Klaus Schöne²

¹ IBA Lifesciences GmbH, Rudolf-Wissell-Str. 28, 37079 Göttingen, Germany

² Sartorius Lab Instruments GmbH and Co.KG, Otto-Brenner-Str. 20, 37079 Göttingen, Germany

Correspondence

E-Mail: mohr@iba-lifesciences.com; klaus.schoene@sartorius.com

Abstract

The enrichment of small extracellular vesicles of endosomal origin (exosomes) with average diameters of less than 150 nm is a prerequisite for the investigation of their exact biological functions. In this application note, an experimental setup is presented, which combines Fab TACS[®] immuno-affinity chromatography based on the Strep-tag[®] technology (IBA Lifesciences), with subsequent filtration using Minisart[®] High Flow syringe filters (Sartorius). We demonstrate that the average hydrodynamic diameter of CD9⁺ or CD81⁺ EVs enriched by affinity chromatography from HEK293 cell culture supernatant or plasma can be effectively reduced by eluate filtration. Thereby, EV populations with a small size distribution (30 – 150 nm) are created. Impurities caused by microvesicles, apoptotic bodies and lipoproteins that other enrichment techniques (e.g. differential and density gradient ultracentrifugation, ultrafiltration and size exclusion chromatography) struggle with, are avoided with our experimental setup.

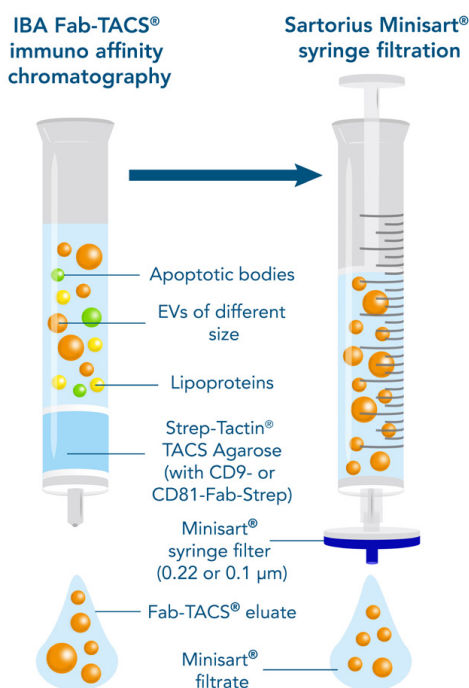
Introduction

Exosomes are small extracellular vesicles (EVs) of endosomal origin and are produced by almost every cell type. They are defined by their biogenesis, and are partially characterized by physiological features, such as the presence of specific surface markers (CD9, CD63 and CD81) or physical characteristics like size and density. EVs with diameters in the range of 30 – 150 nm are classified as small EVs (sEVs) and are of great interest since exosomes also have the same size range. In general, exosomes are derived from early endosomes, by inward budding and subsequent release of the resulting vesicles into the extracellular space (via fusion of a multivesicular body with the plasma membrane). Exosomes support intercellular communication by transferring signals to remote recipient cells. This communication is necessary to maintain cellular functions and tissue homeostasis in all multicellular organisms. Alongside direct cell-cell contact or the transfer of secreted molecules, exosomes constitute an additional important pathway in intercellular communication by serving as carriers for proteins, lipids, RNA and DNA. Because of these properties and their proven importance in numerous physiological and pathological processes, exosomes can be used as biomarkers for diagnosis and prognosis of various disease states. Furthermore, they can be used for therapies, due to their biocompatibility and capacity for signal transfer by the above-mentioned biomolecules. Due to their potential use in clinical applications, exosomes have attracted much attention concerning their roles in health and disease.¹⁻⁴

The enrichment of exosomes is a critical step for investigating their physiological mechanisms and applications in biomedical science. Various techniques have been adopted to facilitate the enrichment of these vesicles. However, since size and density of exosomes overlap with other cellular components, their isolation and analysis can be challenging. Established enrichment techniques are ultracentrifugation, ultrafiltration, size exclusion chromatography (SEC), polymer-based precipitation, and immuno-affinity capture.⁵ For most of these methods, the size of the EVs has an impact on separation and all of them come with different advantages and drawbacks. Thus, a combination of different methods leads to synergetic effects and can improve the enrichment process. In the past, filtration methods were combined with ultracentrifugation. Filtration membranes are used to remove cells and large EVs, and subsequent ultracentrifugation is utilized to separate exosomes from proteins.^{6,7} However, this isolation procedure is time intensive. In addition, it only focuses on physical properties, such as size and density. The main disadvantage of procedures like this is the co-enrichment of non-exosomal material, such as protein aggregates, lipoproteins, macromolecules and microvesicles (MVs).

To overcome impurities caused by size- and density-based EV preparations, immuno-affinity purification techniques have been used to selectively capture exosomes from complex populations by exploiting surface markers like CD81 and CD9.^{5,8} Exosome membranes contain large quantities of these surface protein markers and immuno-affinity chromatography is based on the interaction between these and special selection reagents. Exosomes can be enriched from complex biological mixtures like cell culture supernatants, tissues, and biological fluids by immuno-affinity chromatography. This method is rapid, easy and compatible with standard laboratory equipment, but lacks separation capabilities based on size of already mentioned methods, because it is prone to co-isolate unwanted particles, such as MVs, which carry the same surface markers. Furthermore, most immuno-affinity exosome enrichment reagents (mainly antibodies against the aforementioned surface markers) bind to the surface of isolated EVs, thereby potentially affecting their biological function. Fab-TACS[®] affinity chromatography allows the enrichment of label-free extracellular vesicles, but also cannot prevent the selection of larger, target-marker-positive EVs.

We aimed to develop a protocol combining reversible Fab-TACS[®] immuno-affinity chromatography with sieving effects of Minisart[®] High Flow PES syringe filters with pore sizes of 0.22 µm or 0.1 µm to generate a defined EV product and circumvent the drawbacks of these isolation techniques when used independently.



Methods

The herein presented enrichment of exosomes is based on Fab-TACS® affinity chromatography and subsequent eluate treatment with syringe filters of different pore sizes.

Sample Preparation

HEK293 cell culture supernatant was differentially centrifuged at 300 g and 3,000 g for 10 min, respectively, and filtered using a 0.45 µm Minisart® High Flow PES filter (Sartorius, 16537-K). 10 mL of filtrate was used to conduct the described experiments.

To prepare plasma, buffy coat (BC) was sedimented overnight at 4 °C and the established supernatant was centrifuged twice at 3,000 g for 10 min. Finally, the supernatant was filtered using a 0.45 µm Minisart® High Flow PES filter. 9 mL of pre-treated plasma was used for subsequent experiments.

All reagents were equilibrated to room temperature prior to use. Lyophilized Fab-Streps (IBA Lifesciences, human CD81 Fab-Strep, 6-8015-150 or human CD9 Fab-Strep, 6-8019-150) was dissolved in 1 mL PBS (Gibco™, 20012027) by carefully pipetting up and down. Further, 1 mM Biotin Elution Buffer was prepared by mixing 40 µL of a 100 mM Biotin stock solution (IBA Lifesciences, 6-6325-001) with 4 mL PBS. The Fab-Strep, Biotin Elution and PBS buffers were filtered using 0.2 µm Minisart® NML cellulose acetate filters (Sartorius S6534-FMOSK).

Enrichment and Filtration

The cap of a 1 mL Strep-Tactin® TACS Agarose Column (IBA Lifesciences, 6-6310-001) was removed, and the sealed end of the column was cut at the notch to allow the storage solution to drain. Afterwards, the column was washed by applying 5 mL PBS, before loading the Fab-Strep solution onto the column. After a short incubation (2 min), to allow Fab binding, the column was washed with 5 mL PBS. The pre-treated samples (9 mL of plasma or 10 mL of HEK293 cell culture supernatant, respectively) were applied in steps of 1 mL. After complete sample loading, the column was washed twice with 5 mL PBS to remove unwanted particles and proteins. 1 mL Biotin Elution Buffer was applied and incubated for 5 min to release bound EVs. To complete elution, 3 x 1 mL Biotin Elution Buffer were added.

Each eluate was divided into three aliquots of 1 mL, which were either retained without further treatment, or filtered through a 0.1 µm or 0.22 µm Minisart® High Flow PES syringe filter, respectively (Sartorius, 0.22 µm: 16532-K and 0.1 µm: 16537-K). To confirm that the tested TACS columns and syringe filters do not release particles that could influence concentration and size distribution measurements, the isolation process was also performed using 0.2-µm filtered PBS instead of EV sample. In addition,

1 mL aliquots of PBS were filtered through a 0.1 µm or 0.22 µm syringe filter. All three process controls were analyzed by nanoparticle tracking analysis and no particles were detected (data not shown).

NTA Measurement

To determine particle concentration and size distribution of the samples, nanoparticle tracking analysis (NTA) was performed using the NanoSight NS300 and the software package NTA 3.4 from Malvern (3 movies of 60 s at 25 frames per second, scattering mode, camera threshold: 13, detect threshold: 5, manual fixed focus). For NTA measurements, centrifuged and filtered HEK293 cell culture supernatants were diluted 20:1, whereas Fab-TACS® non-filtered and filtered eluates were diluted 5:1 with PBS. Plasma samples were diluted 400:1 and its eluates 50:1 using PBS as well.

SDS-PAGE and Western Blot

To study the protein composition of isolated EVs from cell culture supernatant, sodium dodecyl sulfate polyacrylamide gel electrophoresis (SDS-PAGE) and western blot analyses were performed. First, EVs were precipitated by mixing an aqueous solution of trichloroacetic acid (10 %, w/v) with the sample in a ratio of 1:1. After vortexing (30 s), the samples were allowed to precipitate on ice for 30 min. Subsequently, precipitates were centrifuged at 5,000 x g for 30 min. The obtained pellet was resuspended in 100 µL PBS and 200 µL 5x SDS loading buffer. The samples were incubated at 80 °C for 5 min and SDS-PAGE was performed at 85 V for 90 min on ice. Blotting to a nitrocellulose membrane was performed with the Trans-Blot® Turbo Transfer System of Bio-Rad (25 V and 1.7 A for 3 min). Then, the blots were blocked for 1 h in 3 % (w/v) BSA-PBS at room temperature. The primary antibodies were diluted 1:1,000 in 3 % (w/v) BSA-PBST and applied overnight at 4 °C on a shaker. The membranes were washed 3 x 5 min with PBST and then the secondary antibody with a dilution of 1:2,000 in 3 % (w/v) BSA-PBST was applied for 1 h at room temperature, while shaking. Finally, the blots were visualized using Western Lightning Plus-ECL reagent (Perkin Elmer) according to the manufacturer's protocol. The blots were analyzed with the Image Lab software (V.6.1) from Bio-Rad. Plasma samples were not analyzed.

Results and Discussion

Fab-TACS® Enables Specific Purification of EVs

We used two different sample types to test our protocol combining immuno-affinity chromatography and filtration: pre-treated HEK293 supernatant and plasma (see sample preparation).

Concerning the supernatant, the starting material contained 16.8 % particles between 30 – 150 nm (data not shown). For the non-filtered CD9- and CD81-specific eluates, proportions of 50 % and 51 % were determined, respectively (Figure 1 A). Using a feed of 10 mL cell culture supernatant, concentrations of 1.62×10^9 and 2.46×10^9 particles/mL in a range of 30 – 150 nm for the CD9⁺ and CD81⁺ eluates were measured, respectively. Considering a

total volume of 4 mL for each eluate, amounts of 6.46×10^9 CD9⁺ and 9.85×10^9 CD81⁺ particles were collected (Figure 1 B). The particles of the pre-treated cell culture supernatant had a mean size (hydrodynamic diameter) of 191 nm (data not shown) and particles of the eluates had mean sizes of 161 nm (CD9⁺ EVs) and 160 nm (CD81⁺ EVs) (Figure 1 C). In summary, an increase of particle counts within the exosome typical size range was achieved through immuno-affinity chromatography. In addition, typical markers for exosomes, Hsp70 and syntenin-1, were detected in all samples (including filtered samples) by western blot analysis, confirming that the detected particles are EVs. Calnexin, as a negative marker for exosomes, was found only in the lysed cell culture (data not shown), but not in the centrifuged and further processed cell culture supernatant (Figure 2).

Figure 1: NTA measurements of Fab-TACS® enriched exosomes using CD9 Fab-Streps or CD81 Fab-Streps from HEK293 supernatant samples ($n = 3$). Proportions of particles in exosomal size range (A), total particle amount (4 mL sample) within this size range (B) and mean particle size of all detected particles (C).

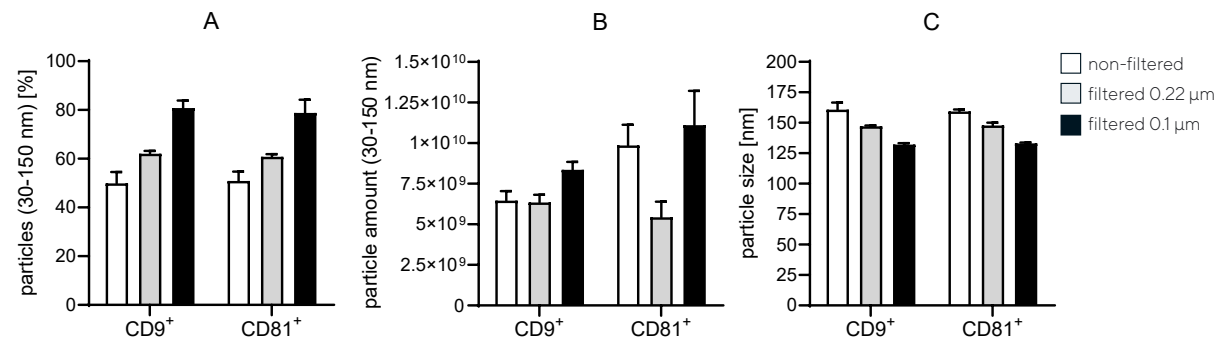


Figure 2: Detection of EV-negative marker calnexin (90 kDa) and EV-positive markers Hsp70 (70 kDa) and syntenin-1 (32 kDa) by SDS-PAGE and western blot analysis.

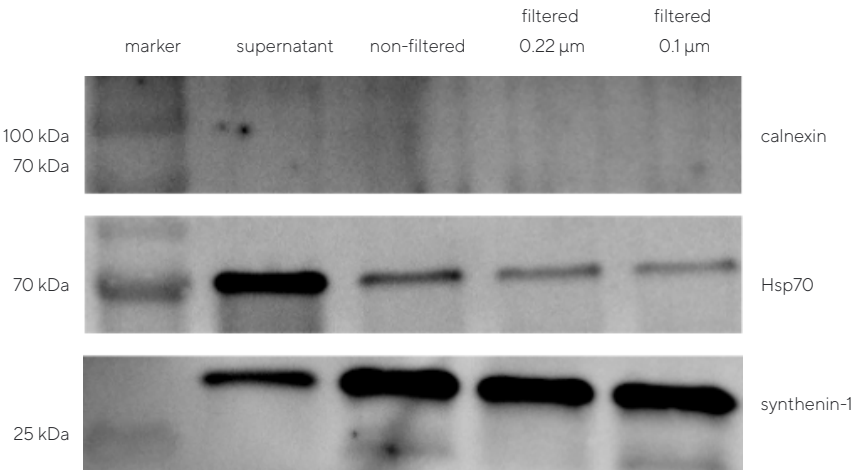
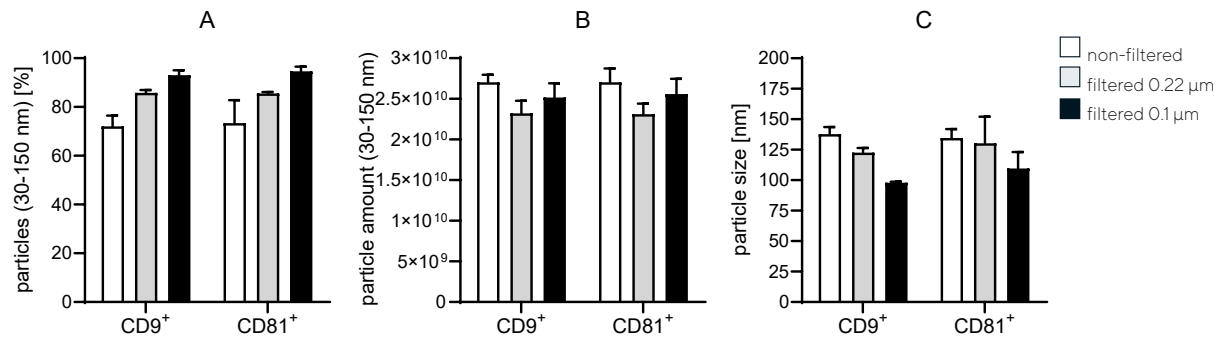


Figure 3: NTA measurements of Fab-TACS® enriched exosomes using CD9 Fab-Streps or CD81 Fab-Streps from BC plasma samples (n = 3). Proportions of particles in exosomal size range (A), total particle amount (4 ml sample) within this size range (B) and mean particle size of all detected particles (C).



According to the enrichment of EVs from cell culture supernatant, the same procedure was conducted using plasma. In comparison to supernatant, 70 % of the particles in the non-filtered CD9⁺ and CD81⁺ eluates were already within the exosomal size range of 30 – 150 nm, assuming that the pre-treated plasma contained more small particles than the supernatant used in this study (Figures 1 A and 3 A). After filtration, the proportion of particles in the desired EV size range increased to 93 % by CD9⁺ enrichment and up to 95 % with CD81⁺ selection. Furthermore, total particle amounts were in the same range for the CD9⁺ and CD81⁺ EV isolation: Yields of approx. 2.5×10^{10} particles demonstrate the high binding capacity of Strep-Tactin® TACS Agarose columns (Figure 3 B).

Minisart® Syringe Filtration Increases the Proportion of Small EVs

The eluates following CD9- and CD81-specific immuno-affinity chromatography of HEK293 and plasma samples were filtered in parallel runs using Minisart® High Flow PES syringe filters, with pore sizes of 0.22 µm or 0.1 µm.

For the non-filtered CD9⁺ HEK eluate a total particle amount of 6.46×10^9 for 4 mL was determined. Amounts of 6.34×10^9 (0.22 µm) and 8.36×10^9 (0.1 µm) were measured after eluate filtration. The treatment with a 0.22 µm filter did not change the particle amount for the CD9⁺ selection to a detectable extent, whereas 0.1 µm filtration led to an increased number of detected particles with regard to the non-filtered eluate (Figure 1 B). Under certain conditions decreasing pore sizes lead apparently to higher particle amounts. Considering the sieving effect, this tendency seems to be contradictory. However, NTA is based on light scattering and is a bulk measurement, which might explain this observation (see explanation of NTA effect below). Nevertheless, an enrichment of smaller particles through filtration was determined by mean particle sizes: For the CD9⁺ samples from HEK supernatant, hydrodynamic diameters of 161 nm (non-filtered), 147 nm (0.22 µm filtered)

and 132 nm (0.1 µm filtered) were detected (Figure 1 C). This is in line with the sieving effect of the Minisart® filters and confirms the enrichment of particles in the exosomal size range (Figure 1 A).

The effects of eluate filtration following selection for CD81⁺ from cell culture supernatant samples were similar: Total amounts of 9.85×10^9 (non-filtered), 5.43×10^9 (0.22 µm) and 1.11×10^{10} particles (0.1 µm) were determined (Figure 1 B). After 0.1 µm filtration the highest particle amount was measured, which was in keeping with the results from CD9⁺ selection. However, a pronounced particle reduction after 0.22 µm filtration was detected for the CD81⁺ eluate. Together with the strong increase after 0.1 µm filtration, it might be concluded that the CD81⁺ eluate contained more large particles after the 0.22 µm filtration, which cause the NTA effect (see below). These particles are more strongly retained by filters with small pore sizes, when compared to filters with larger pores. Mean sizes of these particles were 160 nm for the non-filtered, 148 nm for the 0.22 µm-filtered and 133 nm for the 0.1 µm-filtered sample (Figure 1 C). Thus, as for CD9⁺ selection the filtration of CD81⁺ eluates led to an enrichment of exosome-sized particles.

Like the observed effect in cell culture supernatant, we observed a reduction in particle size by filtration for the plasma samples. The particles of the non-filtered eluate were 138 nm in size after CD9⁺ enrichment and could be reduced to 122 nm (0.22 µm filtration) and 98 nm (0.1 µm filtration). After CD81⁺ enrichment the size was reduced from 135 nm to 130 nm (0.22 µm filtration) and 110 nm (0.1 µm filtration) (Figure 3 C).

The reduction of mean particle sizes was also reflected through the proportions of particles in the exosomal size range. The proportions were 50 % (non-filtered), 62 % (0.22 µm) and 81 % (0.1 µm) for CD9⁺ samples and 51 % (non-filtered), 61 % (0.22 µm) and 78 % (0.1 µm) for CD81⁺ samples (Figure 1 A). Thus, with decreasing pore size,

particles between 30 – 150 nm are more strongly enriched, and therefore probably the proportion of exosomes within the eluted EV population is also increased. The same tendencies concerning size proportions were observed for the enrichment of EVs from plasma (Figure 3 A). In particular, the proportion of particles up to 150 nm was generally higher when the starting material was derived from plasma. Thus, it was easier to refine this sample type to a level where the exosomal size range represented > 90 % of the particle population.

NTA Effect

NTA is based on analysis of scattered light of a bulk of particles. Larger particles have a much higher intensity than smaller particles (data not shown). Therefore, larger particles tend to mask the presence of smaller particles, leading to an underestimation of the concentration of smaller particles in a sample. The use of filters with suitable pore sizes has a positive effect on particle size homogeneity. This is beneficial for particle concentration determination by light scattering methods like NTA. In summary, a more homogenous sample concerning particle sizes will yield more exact results regarding particle concentration.¹⁰ Filtration with 0.1 µm filters resulted in improved homogeneity of the samples and an elevated confidence in the particle concentration, especially in the size range of interest (30 – 150 nm).

Conclusion

The combination of Fab-TACS® immuno-affinity chromatography and Minisart® High Flow PES syringe filtration with pore sizes of 0.22 µm or 0.1 µm enables selective purification of EVs with specific markers such as CD9 and CD81. Regarding size, the proportion of particles with exosomal sizes of 30 – 150 nm can be significantly increased through the filtration step. Larger particles, such as MVs, are depleted to a considerable extent. The process product of CD9 or CD81 immuno-affinity chromatography and 0.1 µm syringe filtration is an EV population which encompasses some important exosome characteristics, like typical surface markers and small hydrodynamic diameters.

References

1. Théry, C. et al. Minimal information for studies of extracellular vesicles 2018 (MISEV2018): a position statement of the International Society for Extracellular Vesicles and update of the MISEV2014 guidelines. *Journal of Extracellular Vesicles* **7**, (2018).
2. Kalluri, R. & LeBleu, V. S. The biology, function, and biomedical applications of exosomes. *Science* **367**, eaau6977 (2020).
3. Zhang, Y., Liu, Y., Liu, H. & Tang, W. H. Exosomes: Biogenesis, biologic function and clinical potential. *Cell and Bioscience* **9**, 1–18 (2019).

4. Pegtel, D. M. & Gould, S. J. Exosomes. *Annual Review of Biochemistry* **88**, 487–514 (2019).
5. Yang, X. X., Sun, C., Wang, L. & Guo, X. L. New insight into isolation, identification techniques and medical applications of exosomes. *Journal of Controlled Release* **308**, 119–129 (2019).
6. Tauro, B. J. et al. Comparison of ultracentrifugation, density gradient separation, and immunoaffinity capture methods for isolating human colon cancer cell line LIM1863-derived exosomes. *Methods* **56**, 293–304 (2012).
7. Gandham, S. et al. Technologies and Standardization in Research on Extracellular Vesicles. *Trends in Biotechnology* **38**, 1066–1098 (2020).
8. Gurunathan, S., Kang, M.-H., Jeyaraj, M., Qasim, M. & Kim, J.-H. Review of the Isolation, Characterization, Biological Function, and Multifarious Therapeutic Approaches of Exosomes. *Cells* **8**, 307 (2019).
9. Yang, X. X., Sun, C., Wang, L. & Guo, X. L. New insight into isolation, identification techniques and medical applications of exosomes. *Journal of Controlled Release* **308**, 119–129 (2019).
10. Maas, S. L. N. et al. Possibilities and limitations of current technologies for quantification of biological extracellular vesicles and synthetic mimics. *Journal of Controlled Release* **200**, 87–96 (2015).

Abbreviations

HEK	human embryonic kidney
RNA	ribonucleic acid
DNA	deoxyribonucleic acid
Fab	antigen-binding fragment
Fab-TACS®	Fab traceless affinity cell selection
PES	polyethersulfone
PBS	phosphate buffered saline
NTA	nanoparticle tracking analysis
BSA	bovine serum albumin
PBST	phosphate buffered saline with 0.01 % (v/v) Tween 20

Germany

Sartorius Lab Instruments GmbH & Co. KG
Otto-Brenner-Straße 20
37079 Göttingen
Phone +49 551 308 0

USA

Sartorius Corporation
3874 Research Park Drive
Ann Arbor, MI 48108
Phone +1 734 769 1600



For further information, visit
[sartorius.com](https://www.sartorius.com)